CLEARED
FOR PUBLIC RELEASE
AFRL/DEO-PA
26 JUL 05

EMP Theoretical Notes

Note 65

25 August 1969

An Improved Shell Model for Computing Neutron-Induced Gamma Dose Rate and Radial Charge Current from a Nuclear Air Burst

Capt Clovis R. Hale
Air Force Weapons Laboratory

Abstract

The usefulness and accuracy of the one-dimensional shell model for computing neutron-induced EMP drivers is extended by application of a gamma-ray buildup factor and a straight-forward method for obtaining average cross-sections. In addition, results from the improved shell model and the previous shell model are evaluated for accuracy by comparison with Monte Carlo and discrete ordinates transport calculations. Graphical results from the improved shell model are given for a number of ranges and neutron source energies.

AFRL/DE 04-433

Contents

List of Figures

List of Tables

TABLE OF SYMBOLS

ϕ	Neutron flux
σ_t	Neutron total reaction cross section
$\delta(t)$	Dirac delta function
t	Time from burst
v	Neutron velocity
x	Distance from origin to shell (see Fig. 1)
D	Gamma Dose build-up factor
C	Radial current build-up factor
u	Distance in mean free paths
b_1, b_2, b_3, b_4,	Parameters of the build-up factor formulas
G	Uncollided gamma flux
k	Gamma total reaction cross-section
c	Velocity of light
w	Distance from source to observer
Q	Dose rate
J	Radial current
r	Distance from origin to observer
B	Gamma production cross-section
U	Gamma flux-to-dose conversion factor
W	Gamma current to radial current conversion factor
e	Electronic charge
σ_{di}	Cross-section for i^{th} ionizing reaction
R	Average range of recoil electron in direction of incident gamma
E_i	Average ionizing energy deposited in the i^{th} reaction
λ_c	Gamma mean free path for Compton collision

TABLE OF SYMBOLS

(Continued)

a	Neutron collision frequency
ν	Gamma collision frequency
$\Delta\nu$	$\nu - a$
ξ	c/v
η	r/vt

I. Introduction

The neutrons emitted from a nuclear air burst interact by inelastic and fast capture collisions with oxygen and nitrogen nuclei in the air to produce a distributed source of high energy gamma guanta. These in turn interact with the constituents of air by Compton, photoelectric, and pair production collisions to ionize the air and produce a net electron current. The resulting dose rate and electron current are referred to as electromagnetic pulse (EMP) sources, since they are the driving terms in Maxwell's equations for computing the electric and magnetic fields. The geometry of this problem is in reality two-dimensional due to the presence of the ground, exponential atmosphere, and curvature of the earth. However, for many problems, adequate results may be obtained by assuming one-dimensional spherical geometry.

The so-called "shell" model is an analytical approximation which accounts for the spatial as well as the time dependence of neutron induced EMP sources. For this model the neutrons are assumed to all occupy a thin spherical shell which expands outward at the neutron velocity. The neutrons interact with air to induce a moving "shell" source of gamma rays, from which the dose rate* and radial electron current are obtained by computing the uncollided gamma flux and current emanating from this source. The total flux or current at a given observer point are obtained by summing the contributions from the source, where the "shell" source is treated as a distribution of infinitesimal point sources. Figure 1 illustrates the geometry of this model. If a unit pulse of neutrons is emitted instantaneously from the burst point, we may represent the gamma source by:

*Here dose rate means the rate at which ionizing gamma energy is deposited in the air. On the average, 34 electron volts of energy are required to form an ion pair, so that one can obtain the ion production rate directly from the dose rate.

Fig. 1 Geometry of the Shell Model

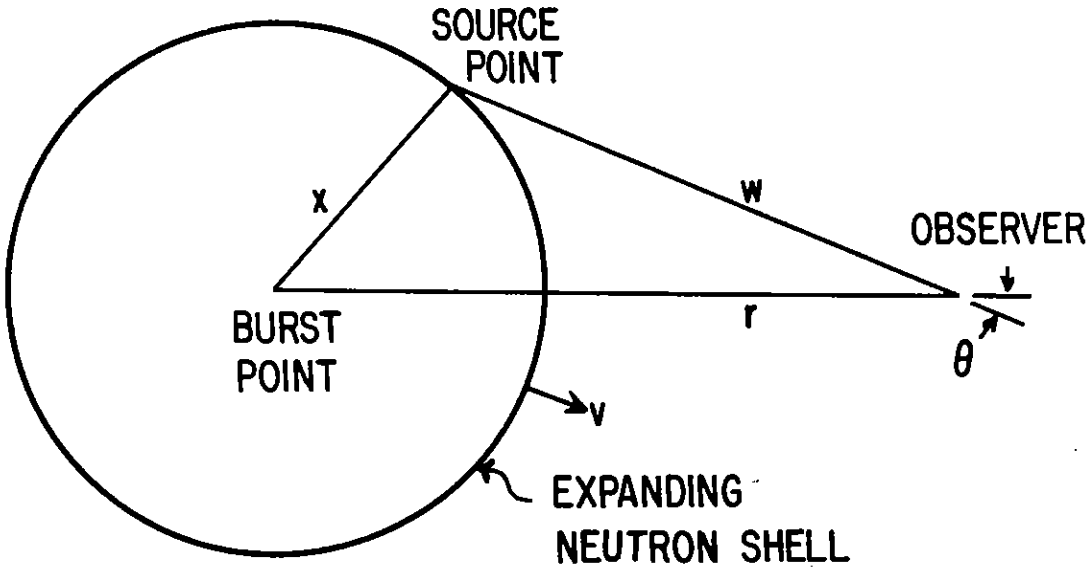

$$S(x,t) = \frac{Be^{-x\sigma_t}\,\delta(t-x/v)}{4\pi x^2}, \qquad (1)$$

Where B = gamma production cross-section.

σ_t = neutron total cross-section.

v = neutron velocity.

$\delta(t)$ = Dirac delta function.

Schaefer has obtained expressions for dose rate and charge current in uniform air based upon the shell model where the source pulse was 2×10^{-8} sec in extent, rather than a Dirac delta function.[1] In addition he obtained parameters for curve fits to these calculations for a 14 MEV neutron source. More recently Moody has extended the model to obtain approximate results for the EMP sources in an exponential atmosphere.[2]

Our purpose in writing this paper is to extend the usefulness of the shell model by accounting for scattered gammas with a buildup factor and to provide a straightforward method for choosing average cross-sections. In addition, the calculations of Schaefer and the present extended shell results will be evaluated for accuracy by comparison to Monte Carlo and discrete ordinates transport calculations.

II. Improved Shell Model

In addition to the features of the shell model described in the introduction, the improved model has two principal elements:

1. The inclusion of a buildup factor to account for the effect of scattered gammas.

2. A straightforward method for obtaining average neutron and gamma cross-sections.

In what follows, we will describe each of those features.

II. A. Buildup Factors

Due to a combination of physical circumstances, it is possible to accurately determine the EMP sources due to scattered gammas by means of steady buildup factors. Stated another way we are assuming that the buildup of dose rate or current at a given observer position due to scattered gamma rays occurs instantaneously. This assumption results in inaccurate results only within the first half-microsecond of gamma arrival time. Here a fast rising pulse is observed, beginning at the uncollided dose (or current) and rising to approximately the steady-state value, then decaying slowly as the source neutrons are attenuated. The detailed structure of the wavefront for the dose rate and radial current are shown graphically in a recent EMP Theoretical Note.[6] The following argument is given to justify the assumption of a steady-state buildup factor.

An analysis by Lelevier[3] of Monte Carlo gamma transport data from a point, pulse source indicates that the time integral of dose rate reaches 70% of its final value in about 10^{-7} sec, while the integral of radial current reaches this value in less than half this time. On the other hand, the neutron-induced gamma source attenuates with approximately a four microsecond time constant. These figures are based upon the assumption of STP air, 14 MEV neutrons, and 3 MEV gammas, which are typical values. Thus, with the lone exception of gamma arrival time, the time history of the EMP drivers due to scattered gammas may be assumed to track the time history of the uncollided gamma dose and current. The discussion here applies strictly to neutron-induced gammas, and not to the prompt gammas from a nuclear burst. Source motion has little effect on the buildup of gamma dose since the most energetic neutrons move only five meters in 10^{-7}sec.

The analytical expression for the buildup factor may take several forms. In a recent survey report Trubey reviewes the various empirical functions used to fit gamma-ray buildup factors.[7] This report also tabulates the energy-dependent

parameters for each of these functions for a variety of materials. Two of these functions were considered for use in the present problem, the linear form and the Berger form.

$$\text{Linear form:} \quad D(u) = 1 + b_1 u \,. \tag{2}$$

$$\text{Berger form:} \quad D(u) = 1 + b_1 u e^{b2u} \,. \tag{3}$$

Where D = dose buildup factor.

u = distance in mean free paths.

b_1, b_2 = curve fit parameters.

Though not indicated in equations (2) and (3) the buildup factor and parameters b_1, b_2 are functions of energy. The radial current buildup factor was assumed to take the same form but with different parameters. Trubey indicates that the linear form is 11% accurate for 2 to 10 MEV sources out to 7 mean free paths, whereas the Berger form is 5% accurate over the same energy range out to 20 mean free paths. These figures are for a water medium which responds like air in the range 1 to 6 MEV since Compton collisions dominate the gamma interactions.

It was decided that the linear form was consistent with other approximations in the model, at least to a range of ten gamma mean free paths, which is about 3km for 5 MEV gamma rays in STP air. Analytical expressions for dose rate and radial current using the linear buildup factor are derived in the appendix. While not used in the numerical results that are presented, the expression for dose rate is also derived using the Berger form for buildup factor.

Parameters for the dose buildup factor were extrapolated from the tabulated water values of Trubey, and parameters for the radial current buildup factor were obtained from the time-integrated radial currents calculated by the discrete ordinates computer code GAMRAN which was programmed by the author.* These parameters

*GAMRAN is a time-dependent discrete ordinates computer code designed for gamma transport in one-dimensional spherical geometry from a point source.

are listed in the next section along with the average cross-sections.

II. B.1 Modified Neutron Cross-Sections

For some finite length of time the neutrons have not scattered appreciably and may be accurately treated with the true reaction cross-section. A measure of this time is the reciprocal of the collision frequency for elastic scatter, which for 14 MEV neutrons in STP air is about 5μs. We observe, however, that neutrons elastically scattered in the forward direction lose at most 13% of their energy, and that elastic scatter for high energy neutrons from either oxygen or nitrogen nuclei is most probable in the forward direction.[4] Thus, a large number of the elastically scattered neutrons continue to move outward, have a velocity close to the velocity of the uncollided neutrons, and occupy a region just behind the moving shell. Having lost little of their energy, they are as capable of producing gamma quanta as the uncollided neutrons. These arguments, of course, apply only to the case of a pulsed source of monoenergetic neutrons from a point. These facts suggest that one might treat a portion of the forward elastic scatter as no reaction, and simply extend the neutron mean free path by an appropriate amount.

Good results were obtained with the extended shell model for 8 to 15 MEV neutrons by integrating the differential scatter cross-section over all forward directions and then subtracting the resulting quantity from the total cross-sections as shown below.

$$\sigma_t' = \sigma_t - \int_0^1 \left(\frac{d\sigma_s}{d\mu} \right) d\mu \qquad (4)$$

Where σ_t' = modified total neutron cross-section.

σ_t = total neutron cross-section.

$\frac{d\sigma_s}{d\mu}$ = differential elastic scatter cross-section.

μ = cosine of scatter angle in the laboratory coordinate system.

For neutrons of energy less than 8 MEV, the gamma production cross-section decreases rapidly with energy. As a result, the loss of energy by elastic scatter reduces the effectiveness of neutrons in this energy range by a greater amount than occurs for higher energy neutrons. To compensate for this loss of effectiveness, the lower limit for the integral in (4) was changed to .3 for neutrons in the range 3 to 8 MEV. Admittedly these choices are somewhat arbitrary. The preceeding arguments are not sufficiently quantitative to define the best choices for cross-sections, but they do establish bounds and indicate trends.

All cross-sections were obtained from the ENDF-B file for oxygen and nitrogen.[5] Air cross-sections for STP air as computed with equation (4) are listed in Table 1. Cross-section units are inverse meters.

Table 1

Modified Neutron Cross-Sections

Neutron Energy MEV	$\sigma_{t'}$
12.2 - 15	4.570×10^{-3}
10 - 12.2	4.547
8.18 - 10	4.066
6.36 - 8.18	4.045
4.96 - 6.36	4.189
4.06 - 4.96	4.474
3.01 - 4.06	5.691

II. B. 2 Gamma Cross-Sections

One method of dealing with the profusion of gamma energies produced by neutron inelastic and fast capture collisions is to do a number of shell

Fig. 2 R^2 times initial dose. Exponential curve fit for obtaining average gamma cross-section and equivalent gamma energy.

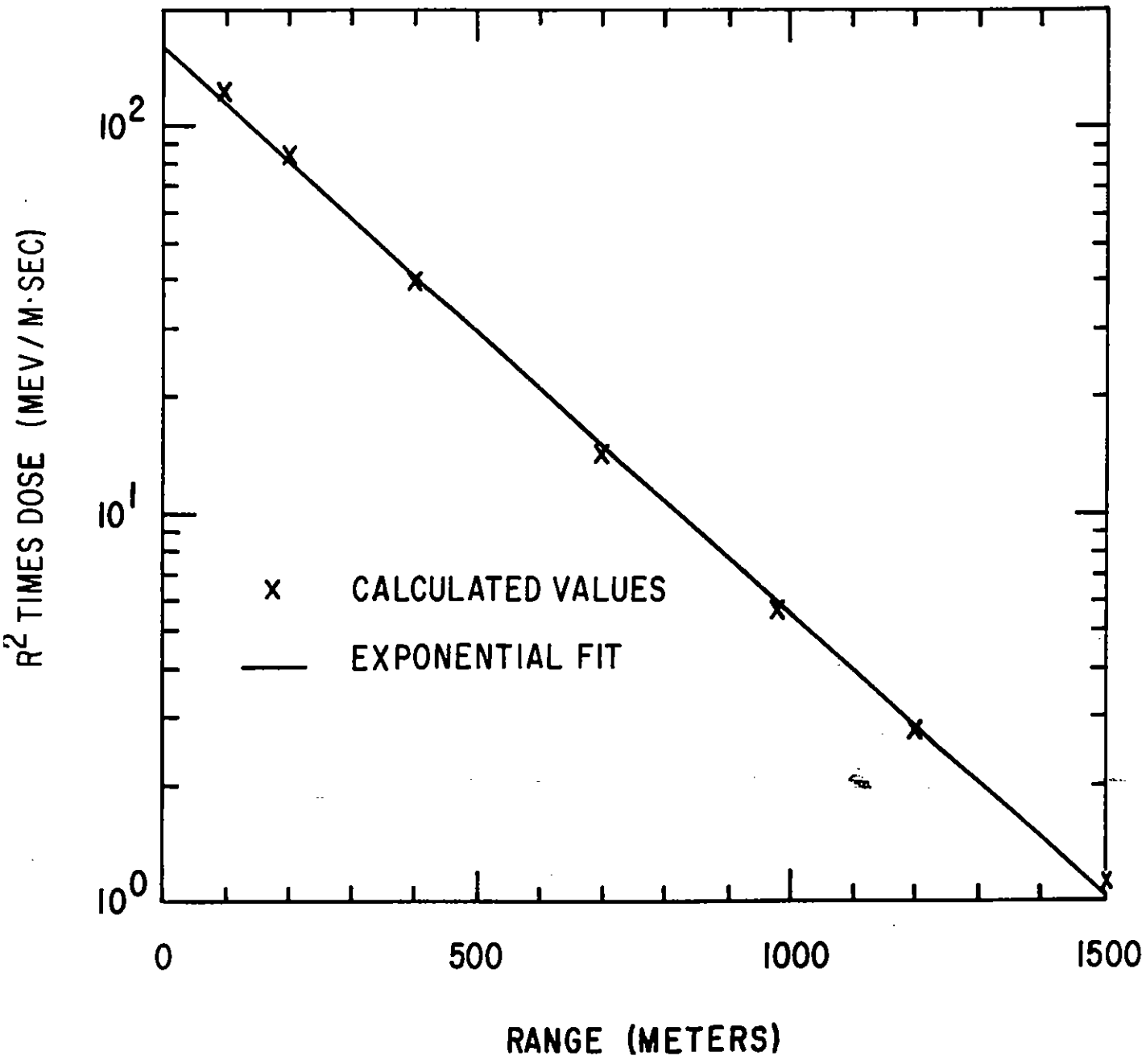

calculations, one for each gamma energy (or narrow energy band). We seek, however, to do the minimum number of calculations consistent with acceptable accuracy. In what follows, a method is developed for selecting a single equivalent gamma energy and the associated shell model parameters. For convenience, these are listed and defined below.

B = gamma production cross-section.

k = gamma total reaction cross-section.

U = gamma flux-to-dose conversion factor.

W = gamma current to electron current conversion factor.

b_1= slope of linear dose buildup factor.

b_3= slope of linear radial current buildup factor.

$\bar{E}$ = equivalent gamma energy.

It is possible to calculate precisely the magnitude of the dose rate at the gamma arrival time, if cross-sections for gamma production are precisely known.

$$4\pi r^2 \, Q(t=r/c,r) = v \sum_{i=1}^{N} B_i U_i e^{-k_i r} \qquad (5)$$

Where Q = dose rate.

r = range.

v = neutron velocity.

N = total number of gamma energies produced.

i = subscript designation of the gamma energy dependence.

The function $4\pi r^2 Q$ is plotted on log-linear paper out to the largest distance of interest and then a single straight line is drawn through the points, as illustrated in Fig. 2. This "eyeball" fitted straight line determines the quantity k and the single equivalent gamma energy $\bar{E}$ is selected as the gamma energy corresponding to a total reaction cross-section k. The quantities b_1, b_3, U, and W are chosen to be those which correspond to gamma energy $\bar{E}$. The equivalent gamma

TABLE 2

AVERAGE GAMMA PARAMETERS

Neutron Energy, MEV	$\bar{E}$ MEV	B m^{-1}	k m^{-1}	U MEV·m^{-1}	W Amps	b_1	b_3
12.2 - 15	5.00	3.83×10^{-3}	3.330×10^{-3}	1.108×10^{-2}	3.90×10^{-21}	.495	.370
10 - 12.2	4.83	3.85	3.396	1.056	3.81	.508	.375
8.18 - 10	4.70	2.39	3.454	1.034	3.75	.516	.378
6.36 - 8.18	4.25	1.42	3.638	.961	3.51	.563	.395
4.96 - 6.36	3.89	.332	3.795	.907	3.30	.600	.412
4.06 - 4.96	2.45	.0926	4.905	.676	2.31	.890	.540
3.01 - 4.06	2.43	.0326	4.950	.675	2.28	.896	.546

production cross-section is selected in a way that preserves the rate of total gamma energy production as follows:

$$\text{Let } F = \sum_{i=1}^{N} B_i E_i, \tag{6}$$

where E_i = gamma energy corresponding to B_i.

Then $B = F/\bar{E}$.

The parameters tabulated in Table 2 are based upon an "eyeball" fit to the arrival time gamma dose rate as described above over the range zero to 1500 meters. However, it will be shown later that calculations using these parameters provide accurate results out to a range of at least 2000 meters for neutron sources in the range 8 to 15 MEV. The gamma production cross-sections were extracted from a set of group-averaged cross-sections which utilized 22 neutron groups and 18 gamma groups. The term "group" may be interpreted "energy band." The neutron groups were distributed over the energy range thermal to 15 MEV, while the gamma energy groups were spread over the range .02 to 10 MEV. Neutron cross-sections for this set were derived from the ENDF-B[5] file, while gamma production cross-sections were obtained from many sources. A more complete description of these cross-sections is given in reference 9. The flux-to-dose factors were computed from the mass attenuation coefficients for energy absorption in air tabulated in reference 10. The electron current was assumed to be proportional to the gamma current, with the proportionality factor

$$W(E) = eR(E)/\lambda_c(E) \tag{8}$$

Where e = electronic charge.

$R(E)$ = electron average forward range.

λ_c = mean free path for Compton collisions.

Values of R(E) in air were obtained from a semi-emperical development by W.R. Graham.[14] Lastly, the source of buildup factor parameters b_1, b_3, was given in the previous section.

III. Discussion of the Validity of Solutions Based Upon a Dirac Delta Source

Due to the added feature of the gamma buildup factor, it was necessary to redevelop the shell model expressions for Q (dose rate) and J (radial charge current), which is done in the appendix. These expressions, numbers (26) and (27), are based upon an infinitely thin shell source and a linear gamma buildup factor. The development was carried one step further than previously reported, resulting in solutions in terms of exponential integrals. These expressions are readily adaptable to doing a convolution integral with point sources that are extended in time, and in fact, this appears to be the most straightforward way of treating the singularity in Q and J that occurs at neutron arrival time.

The shell model solutions based upon a Dirac delta function source predict infinite values for Q and J at time $t = T_o$, where $T_o = r/v$, the neutron arrival time. The singularity is logarithmic and therefore easily removed for any source finite in extent. In particular, values for Q and J at $t = T_o$ were computed by doing a convolution integral on expressions (26) and (27) for a source of length Δt and amplitude $1/\Delta t$. To carry this out, use was made of the properties of exponential integrals of small arguments, and resulted in the approximate expressions (33) and (35). The reader is referred to the appendix for the details of this development.

A question that could now be asked is, "Under what conditions can the expressions based upon a Dirac delta source be used directly for calculating Q and J which result from a source which is extended in time?" Moody developed a theory for conservative bounds on this question, as summarized below.[2] For a shell thickness of one meter, the conditions are:

$$r > 100 \text{ meters} \tag{9}$$

$$|t - T_o| > 10^{-7} \text{sec.} \tag{10}$$

That is, if the observer is at least 100 meters from the origin (source), and

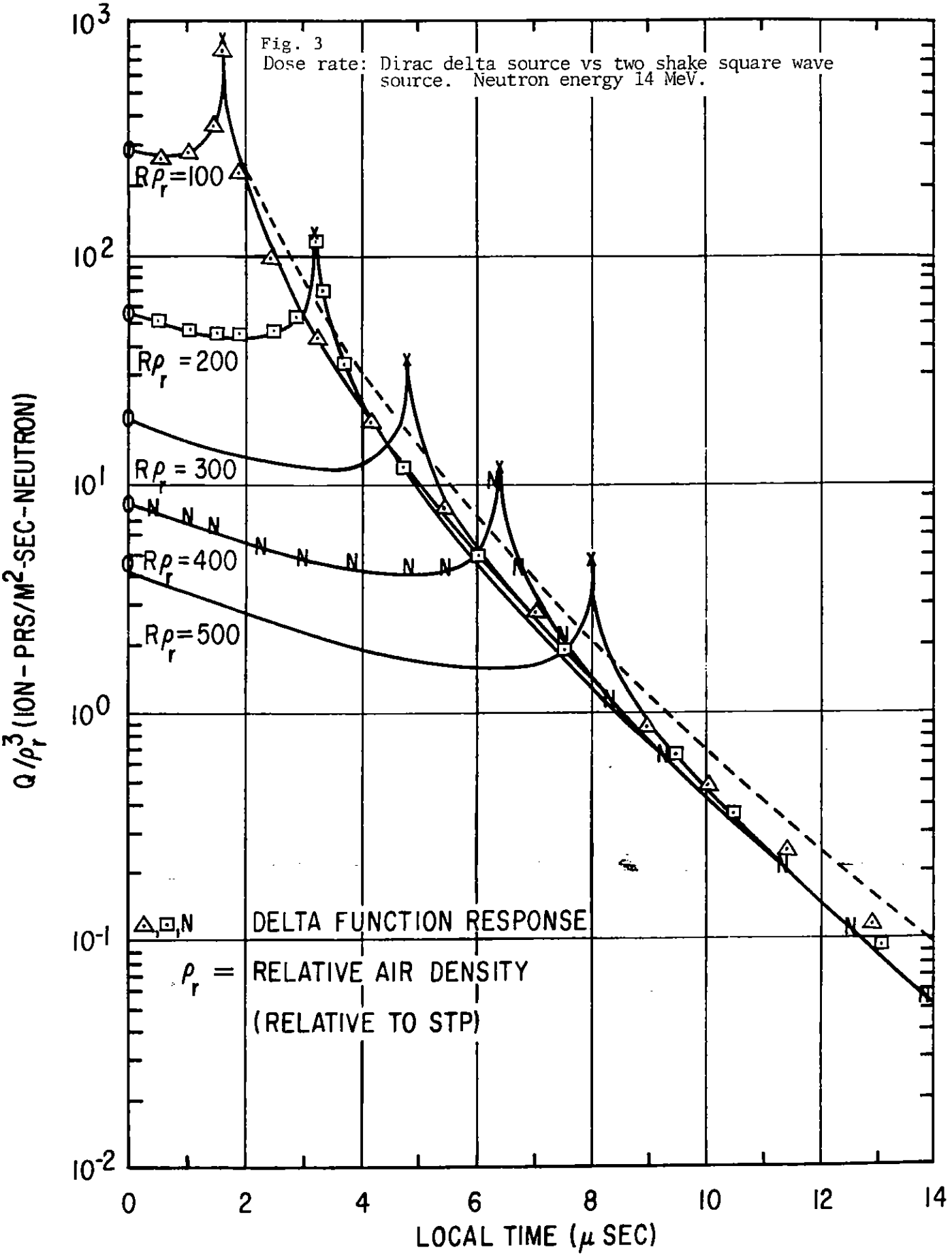
Fig. 3
Dose rate: Dirac delta source vs two shake square wave source. Neutron energy 14 MeV.
10^3
10^2
10^1
10^0
10^{-1}
10^{-2}
$R\rho_r$=100
$R\rho_r$ =200
$R\rho_r$ = 300
$R\rho_r$=400
$R\rho_r$=500
Q/ρ_r^3 (ION-PRS/M^2-SEC-NEUTRON)
△,□,N DELTA FUNCTION RESPONSE
ρ_r = RELATIVE AIR DENSITY
(RELATIVE TO STP)
0
2
4
6
8
10
12
14
LOCAL TIME (μ SEC)

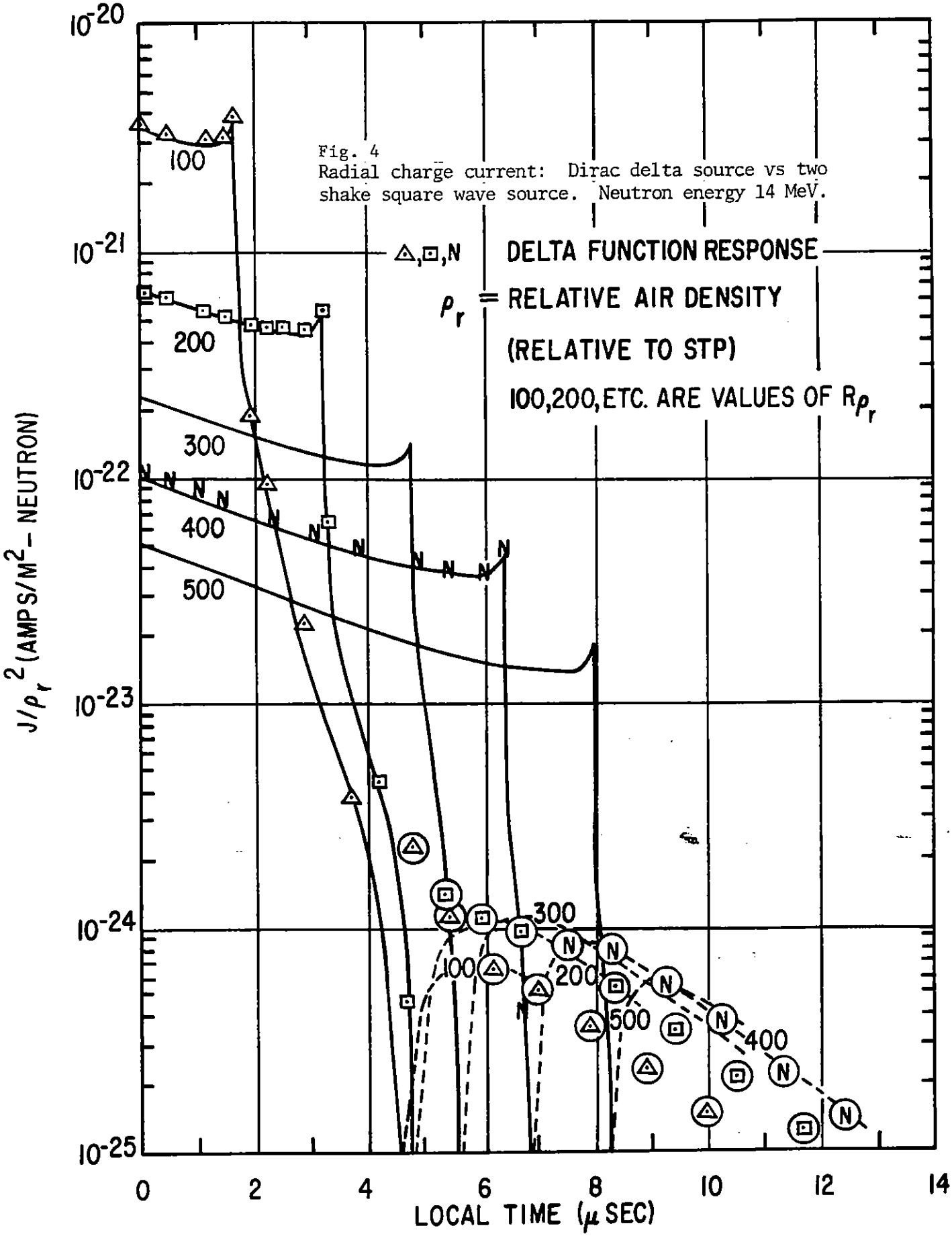

Fig. 4
Radial charge current: Dirac delta source vs two shake square wave source. Neutron energy 14 MeV.

t is more than 10^{-7} sec from T_o, the infinitely thin shell expressions are valid for the finite shell source. It should be noted that a one meter shell is the result of a square 2×10^{-8} sec pulse source of 14 MEV neutrons.

Rather than pursue this question further in a theoretical sense we merely present calculated results to show that (9) and (10) are reasonable sufficiency conditions so that expressions (26) and (27) may be used with confidence. Figs. 3 and 4 are a reproduction of Schaefer's result[1] for a 2×10^{-8} sec source pulse, with calculated values from the expressions derived in this paper overlaid in the form of symbols. Expressions (33) and (35) were used to compute the values of Q and J at neutron arrival time, where Δt in the formulas was set to 2×10^{-8} sec. Clearly, the two results are indistinguishable. Thus, other calculations presented in this paper will follow the same pattern, using expressions derived in the appendix.

For reference, the parameters used in the above calculation are listed in Table 3. These are the parameters suggested by Schaefer, written in the terminology of this paper. They were based upon an assumed neutron energy of 14 MEV and a gamma energy of 7 MEV.

Table 3

Shell Model Parameters Suggested by Schaefer

$\sigma_t = 5.0 \times 10^{-3}$ m^{-1}	$U = 3.34 \times 10^{2}$ ions pairs/m
$k = 2.5 \times 10^{-3}$ m^{-1}	$W = 4.06 \times 10^{-21}$ amps
$\beta = 2.7 \times 10^{-3}$ m^{-1}	$\Delta t = 2 \times 10^{-8}$ sec
$v = 5.2 \times 10^{-7}$ m/sec	$b_1 = 0$
	$b_3 = 0$

It should be noted that we have not completely answered the question posed above to the extent of producing necessary conditions. However, the sufficiency conditions (9) and (10) are adequate to our purposes in this paper.

IV. Accuracy of Results

Recent Monte Carlo[11,12] (MC) and discrete ordinates[13] (SN) transport calculations have made it possible to evaluate the simple transport models used in the past, such as the presently investigated shell model. The MC calculation was for an air over ground geometery, with the burst point at the interface. The ground was treated as an absorber for neutrons and as very dense air for gamma rays. The SN results were for a medium of uniform air. Neutron cross-sections for both calculations were taken from the ENDF-B file.[5] The same set of group averaged cross-sections discussed in section II.B.2 were used in the SN calculation. One would expect the MC result to be lower than the SN result because of ground absorption, and this is the case as indicated in Figures 6 to 11. The two transport calculations, SN in a medium of homogeneous air, MC with source at the air-ground interface, were selected to illustrate the extent of usefulness of the shell models over the greatest range of problems to which they might be applied.

Two other observations should be mentioned here. The shell model prediction for both dose rate and radial current is invalid after passage of the neutron wave. The reason for this is that the gamma source from scattered neutrons is unaccounted for by the shell model for an observer within the neutron shell. This would be position B in Fig. 5. On the other hand, a method was indicated in section II.B.1 to partially account for the gamma source from scattered neutrons seen by an observer at A by lengthening the mean free path of the uncollided neutrons. As the results will show, this is successful, because

Fig. 5 Gamma source as seen by observers inside and outside the moving shell of neutrons.

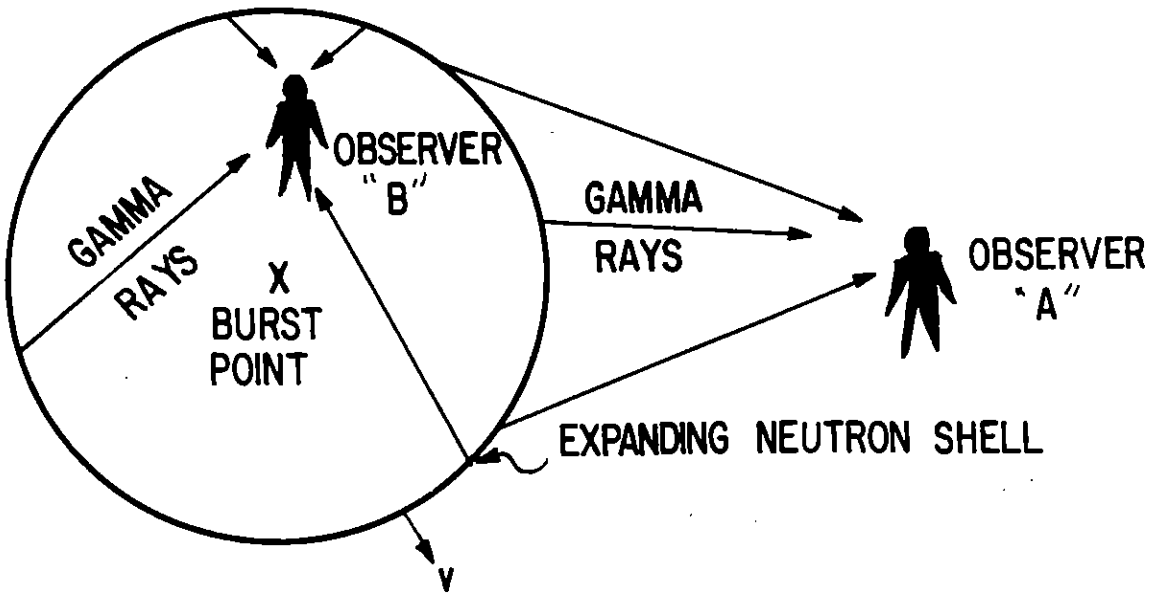

Fig. 6 Dose rate at a range of 580 meters, source energy 12.2 - 15 MeV. Shell models vs Monte Carlo and discrete ordinates

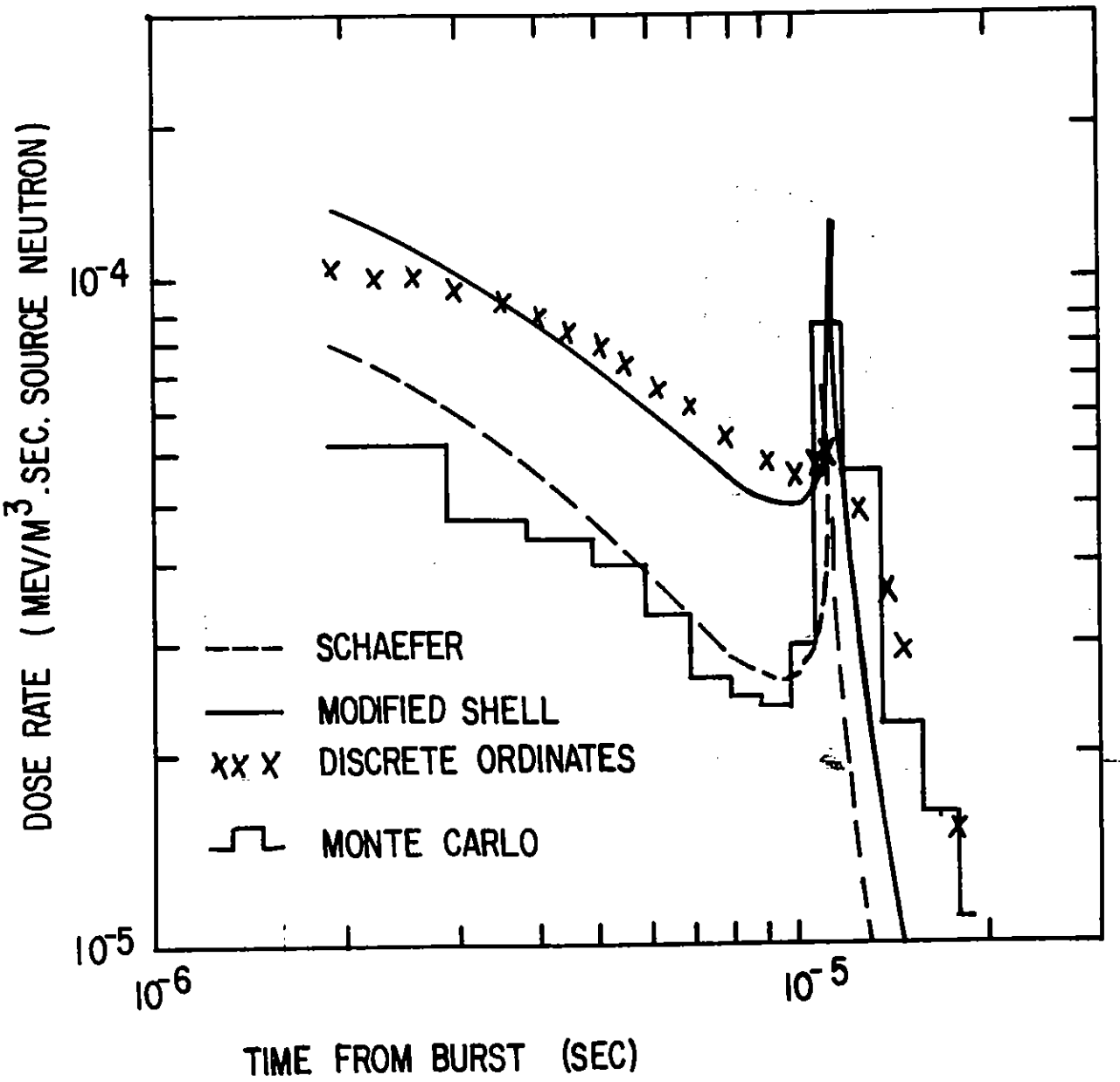

Fig. 7 Radial current at a range of 580 meters, source energy 12.2 - 15 MeV. Shell models vs Monte Carlo and discrete ordinates.

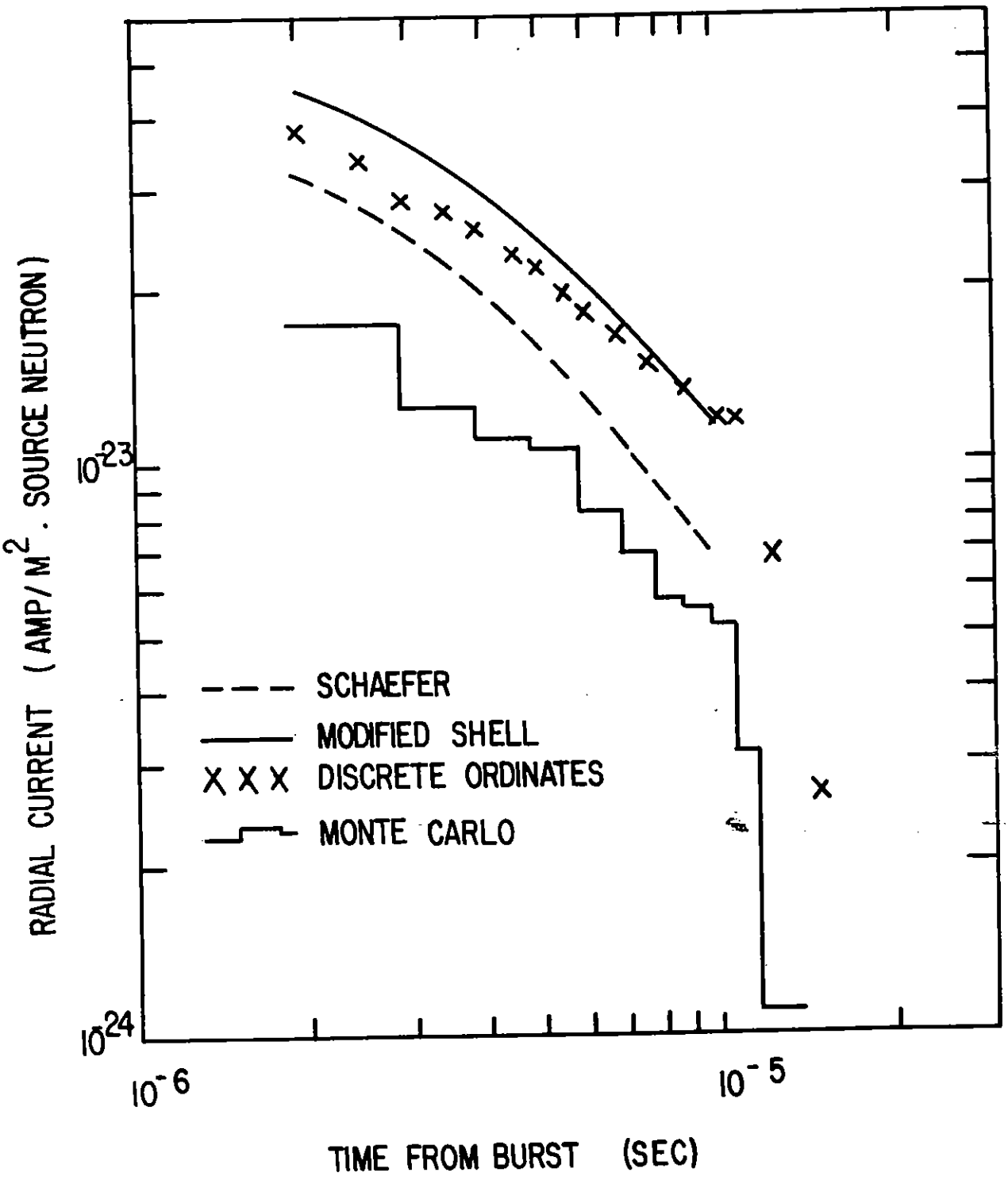

Fig. 8 Dose rate at a range of 980 meters, source energy 12.2 - 15 MeV. Shell models vs Monte Carlo and discrete ordinates

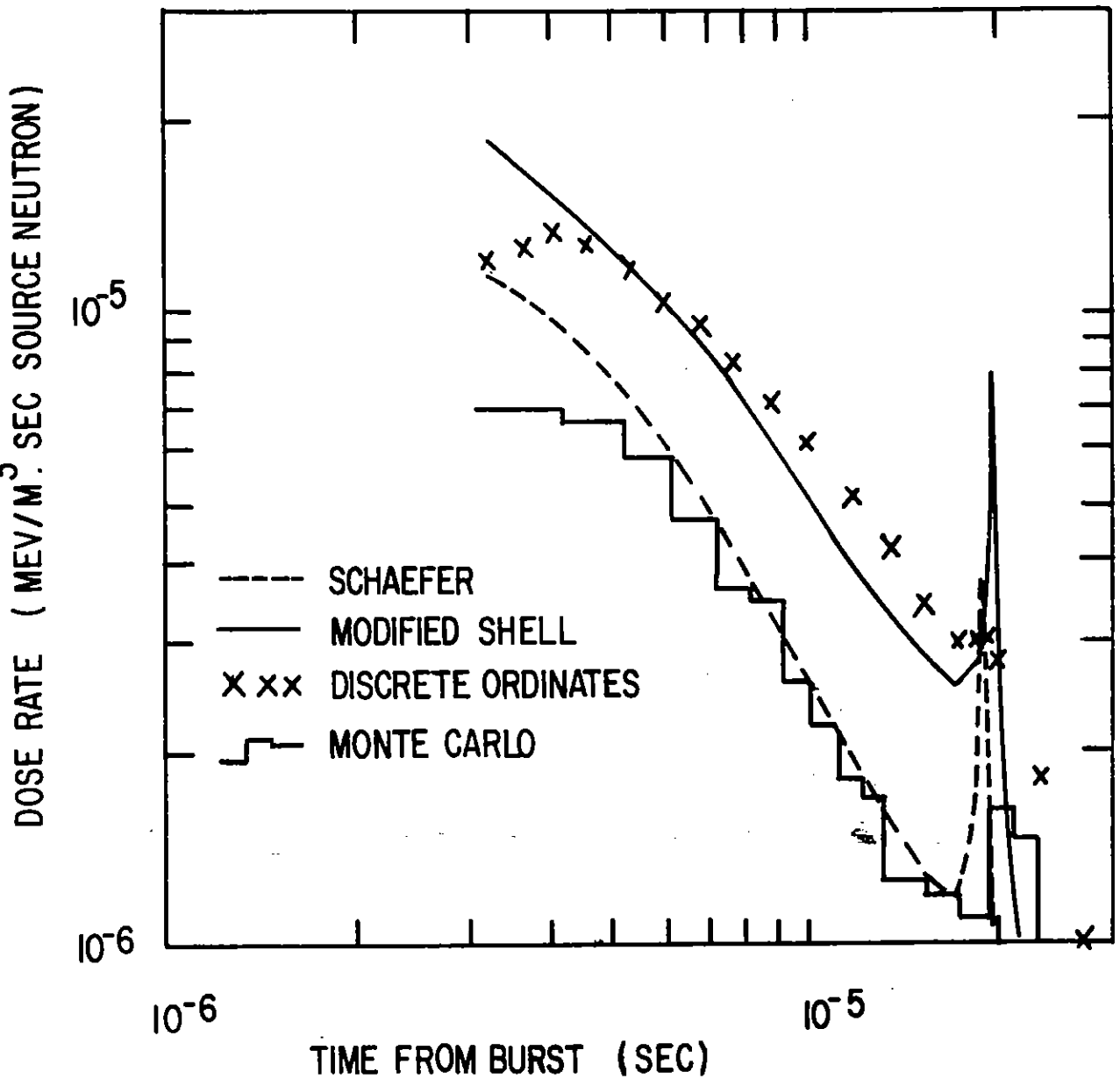

Fig. 9 Radial current at a range of 980 meters, source energy 12.2 - 15 MeV. Shell models vs Monte Carlo and discrete ordinates

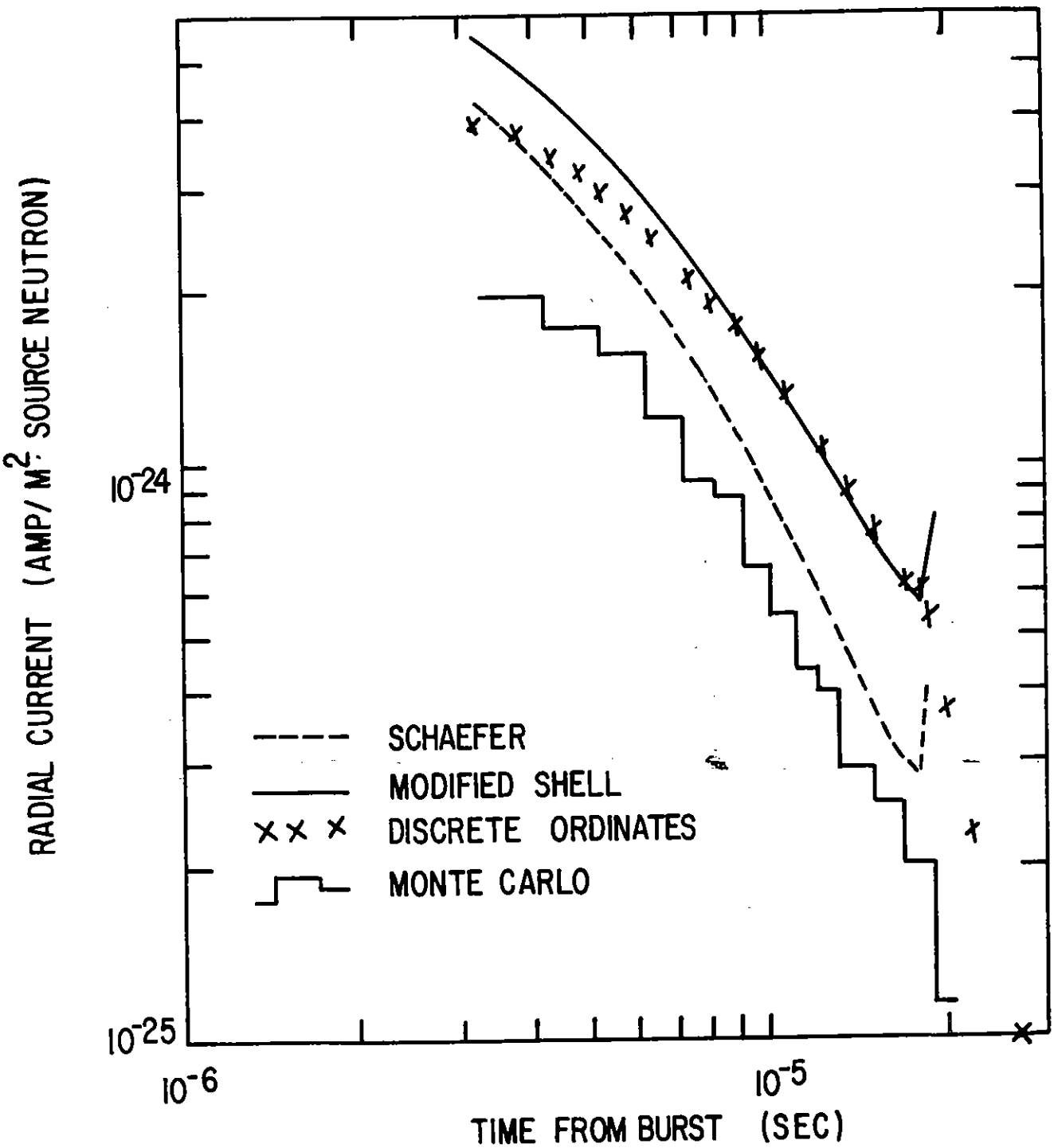

Fig. 10 Dose rate at a range of 1950 meters, source energy 12.2 - 15 MeV. Shell models vs Monte Carlo and discrete ordinates

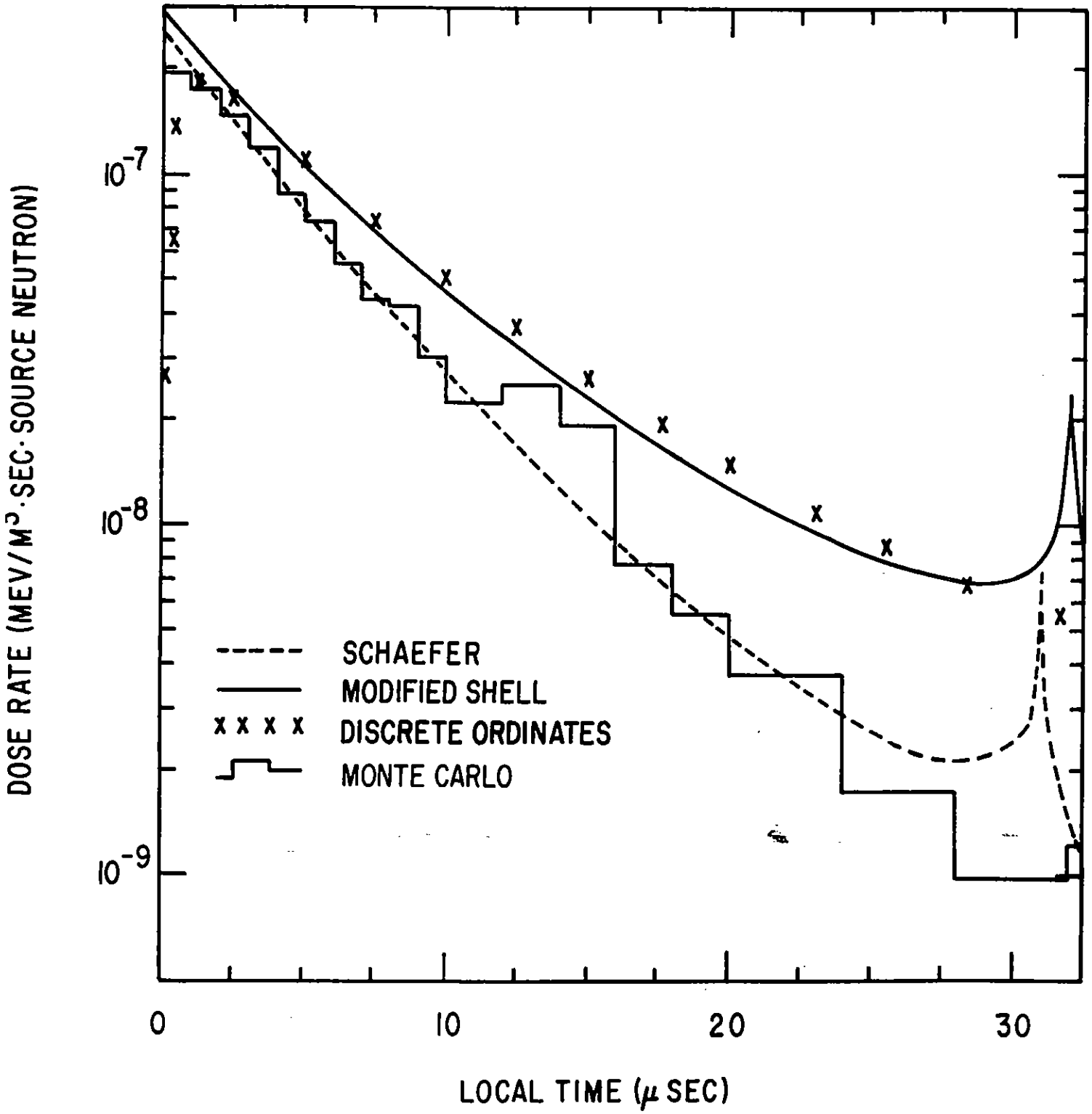

Fig. 11 Radial current at a range of 1950 meters, source energy 12.2 - 15 MeV. Shell models vs Monte Carlo and discrete ordinates

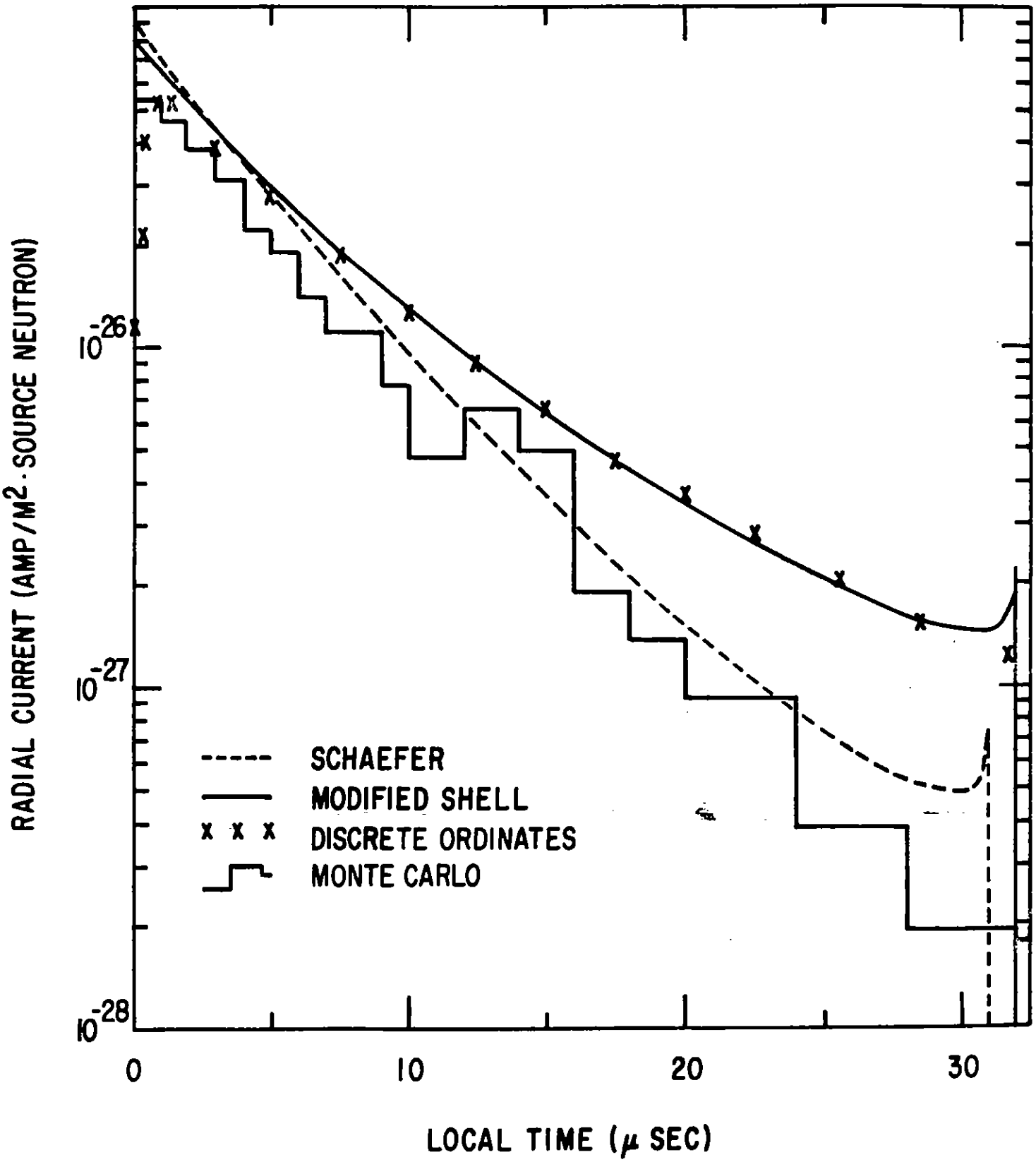

to an observer at A the spatial distribution of scattered neutrons is acequately treated by lumping them into the moving shell. For an observer within the shell, the spatial distribution of the gamma source cannot be treated in this crude way. The other point is that neigher the MC, SN, or shell methods accurately predict the dose rate or charge current within the first half microsecond of gamma arrival, at which time a fast rising pulse should be observed, due to the buildup of scattered gamma rays. This is due to insufficient time resolution in the case of MC and SN, and to the lack of a time dependent buildup factor in the case of the shell models. With these last two observations in mind, we will make quantitative comparisons only for the time range from a half microsecond after gamma arrival to a microsecond before neutron arrival.

Figs. 6 to 11 compare the MC, SN, Schaefer shell (SS), and modified shell (MS) results for dose rate and radial current at the three representative ranges, 580 meters, 980 meters, and 1950 meters. Neutron source spectrum for each of these is nominally a uniform band 12 to 15 MEV or monoenergetic at or near 14 MEV. The MC result is for an observer at the air-ground interface, where the maximum effect from ground absorption should be observed. Cross-sections and other parameters for the SS calculation taken from reference 1 were listed in section III. We have already shown that shell model results from a Dirac delta source are equivalent to results from a two shake* pulse source. For this reason a delta function source was used in all shell model calculations, SS as well as MS.

The relative differences in results from the four computational methods are displayed in table 4. Each value listed is the ratio of values from two methods taken at the point of maximum relative difference. Thus, the average difference is always less than indicated by this listing.

*one shake= 10^{-8} sec.

Table 4

Comparison of Four Calculational Techniques at the Point of Maximum Relative Difference

Range, Meters	Quantity	SS/MC	SS/SN	MS/SN
580	Q	1.30	.45	1.18
	J	1.70	.56	1.17
980	Q	1.10	.38	1.28
	J	1.80	.45	1.20
1950	Q	1.00	.33	1.20
	J	1.30	.33	1.25

We note that the MC and SS agree to within 30% for Q and to within less than a factor of two for J, and that agreement both in value and curve shape improve with increasing range. The SS and SN values differ by at most a factor of 3 and the difference worsens with increasing range. The modified shell and discrete ordinates differ by no more than 30% for both Q and J at all ranges listed in table 4.

Since it is beyond the scope of this paper to investigate the effect of the ground on EMP drivers, we have not discussed the differences in the SN and MC results. To fully explore the differences in these calculations would require a detailed correlation of cross-sections and estimates for the effect of assumptions made in the MC calculation to treat neutron and gamma transport in the ground.

The modified shell and SN results were also compared for other neutron energies, and the agreement indicated above is true for the MS results at neutron energies 8 to 15 MEV. If the range is limited to 1000 meters, or local time is limited to 30 μs, the MS and SN differ by at most 40% for neutron source energies 3 to 8 MEV. Typically, the difference is 10-20% in this range. Beyond the above bounds, differences of up to a factor of 8 occur. Beyone 2000 meters, the shell

results are probably not reliable for the source energy range 3 to 6 MEV. This is of course for STP air density, and the bounding distances scale inversely with density.

V. Modified Shell Calculated Results

The accuracy of the modified shell results, as compared to those of a discrete ordinates calculation was discussed in the previous section. These results are displayed graphically for a number of ranges from 100 to 3000 meters and neutron energies from 3 to 15 MEV in Figs. 12 to 25. The results may be scaled to air densities other than STP by the method indicated in Ref. 6.

VI. Summary

The accuracy and useful range of the shell model may be extended by the inclusion of a gamma-ray buildup factor and by careful selection of the neutron and gamma average cross-sections. Calculated results using the improved shell model are in disagreement with results from a discrete ordinates calculation by at most 30% over a wide range of penetrations and source energies. The Schaefer result agrees well with a Monte Carlo calculation in which both source and observer are at the air-ground interface, but differs by as much as a factor of 3 with the SN result, which was for homogeneous air.

VII. Acknowledgments

This work was accomplished by the author while doing research at the Air Force Weapons Laboratory toward completion of the requirements for the degree of Doctor of Science from the Air Force Institute of Technology. I wish to thank Prof. C. J. Bridgman for his advice and for his participation in several stimulating discussions. Thanks are also due Rodney Lowen for doing most of the required computer programming.

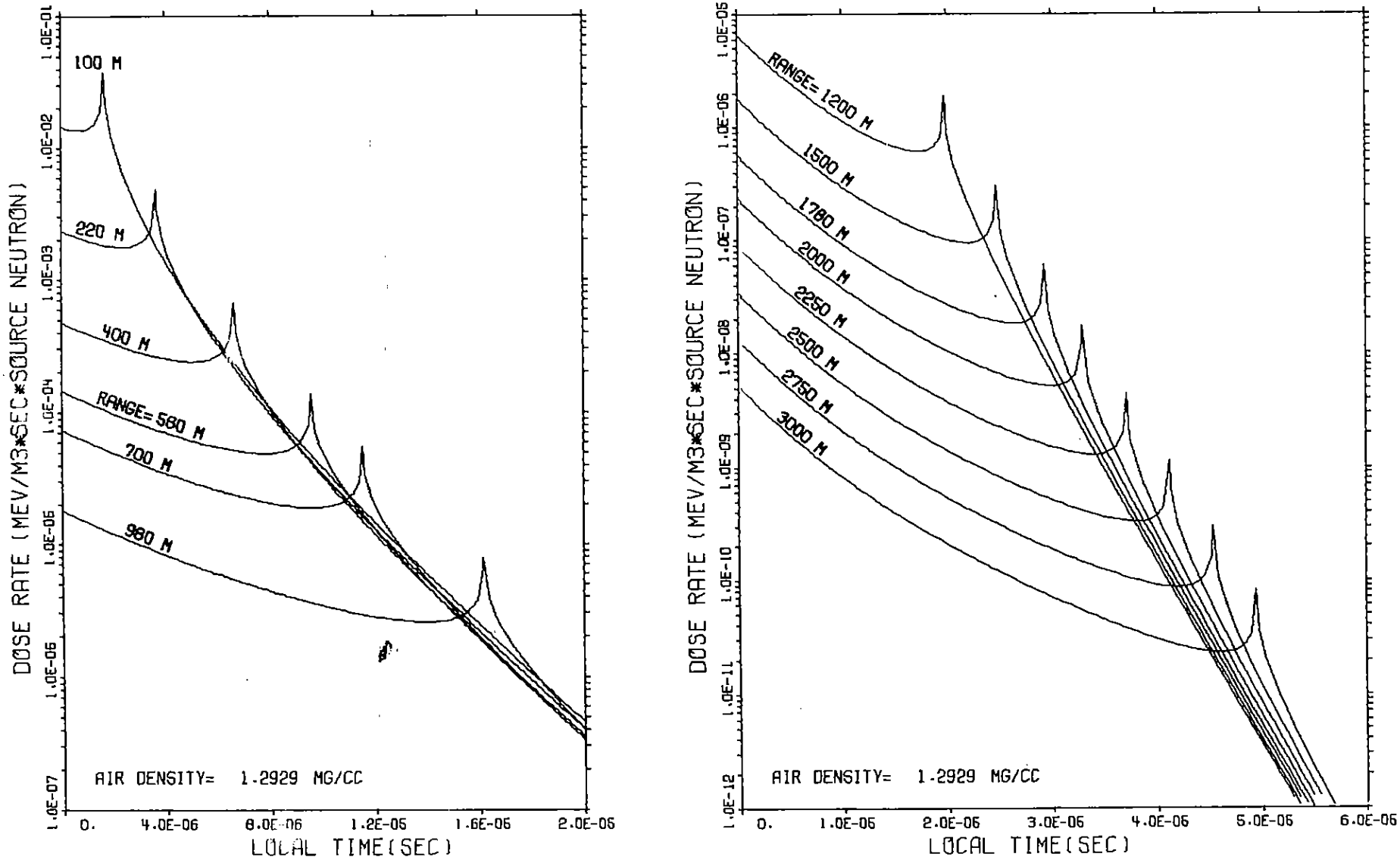

FIG. 12 GAMMA DØSE RATE
NEUTRØN SØURCE ENERGY= 12.20 TØ 15.00 MEV

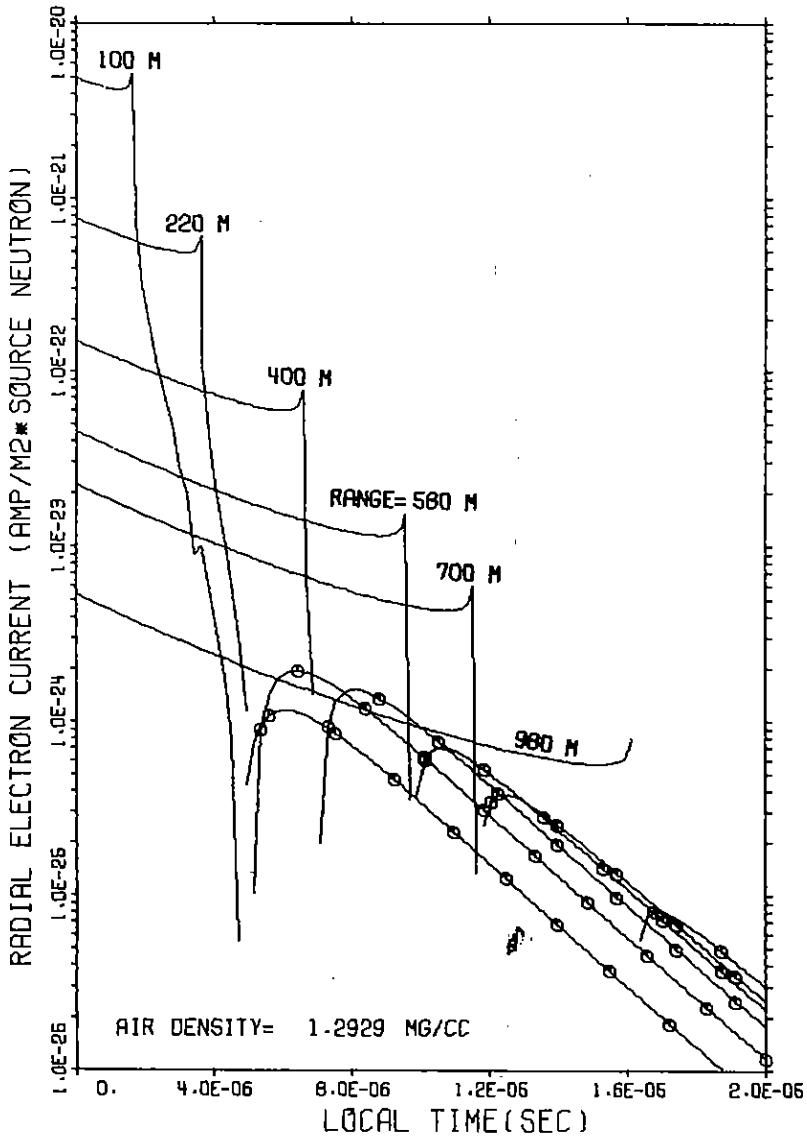

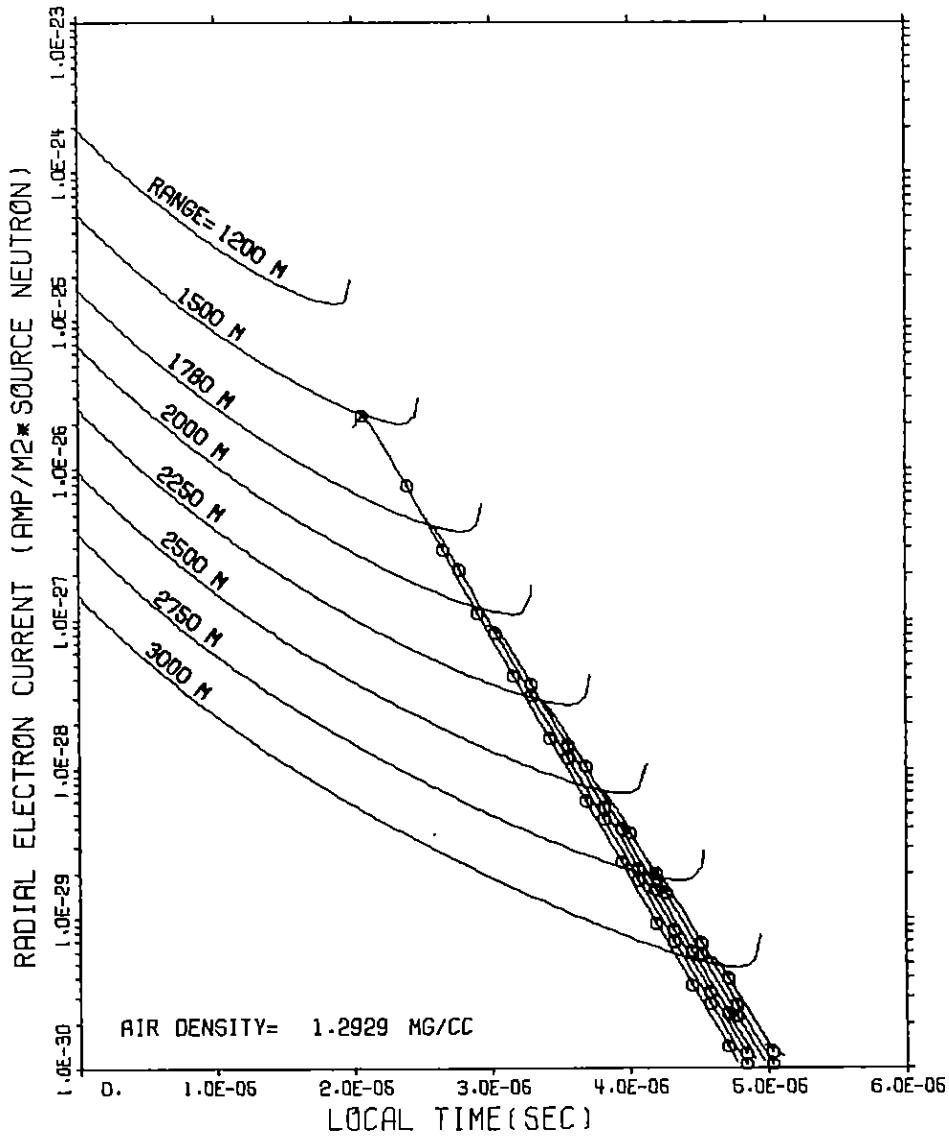

FIG. 13 RADIAL ELECTRON CURRENT
NEUTRON SOURCE ENERGY= 12.20 TO 15.00 MEV

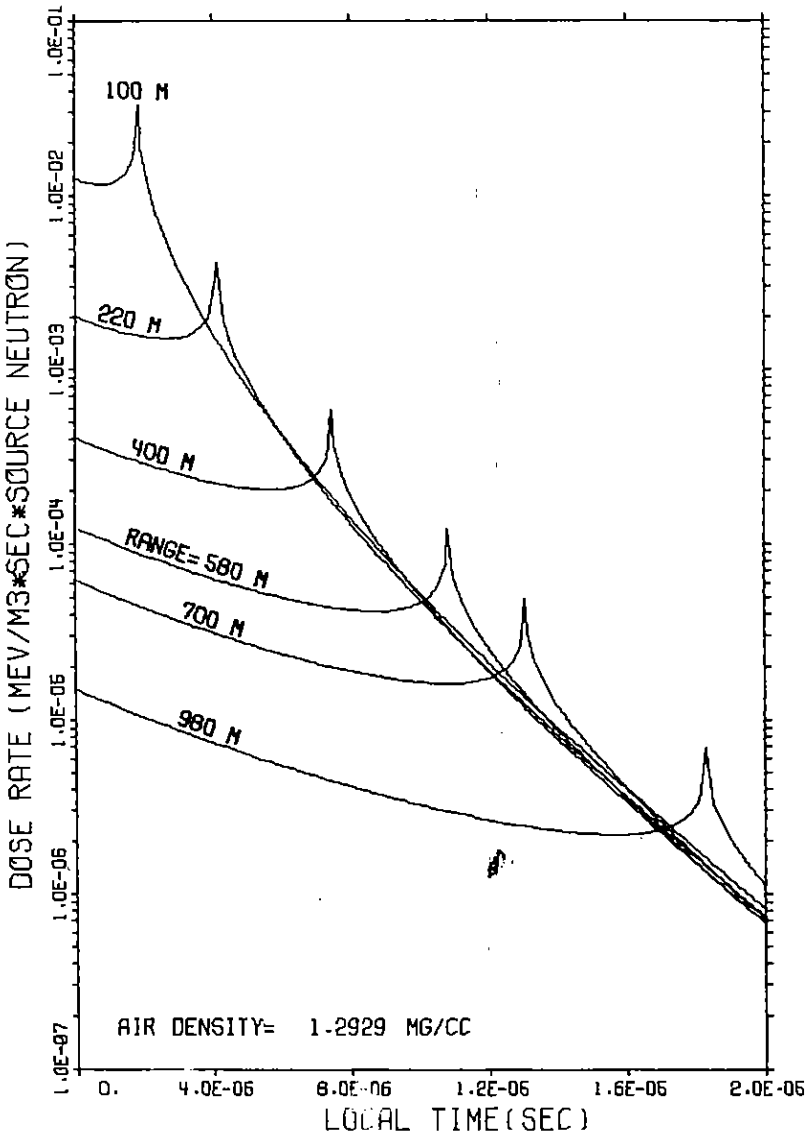

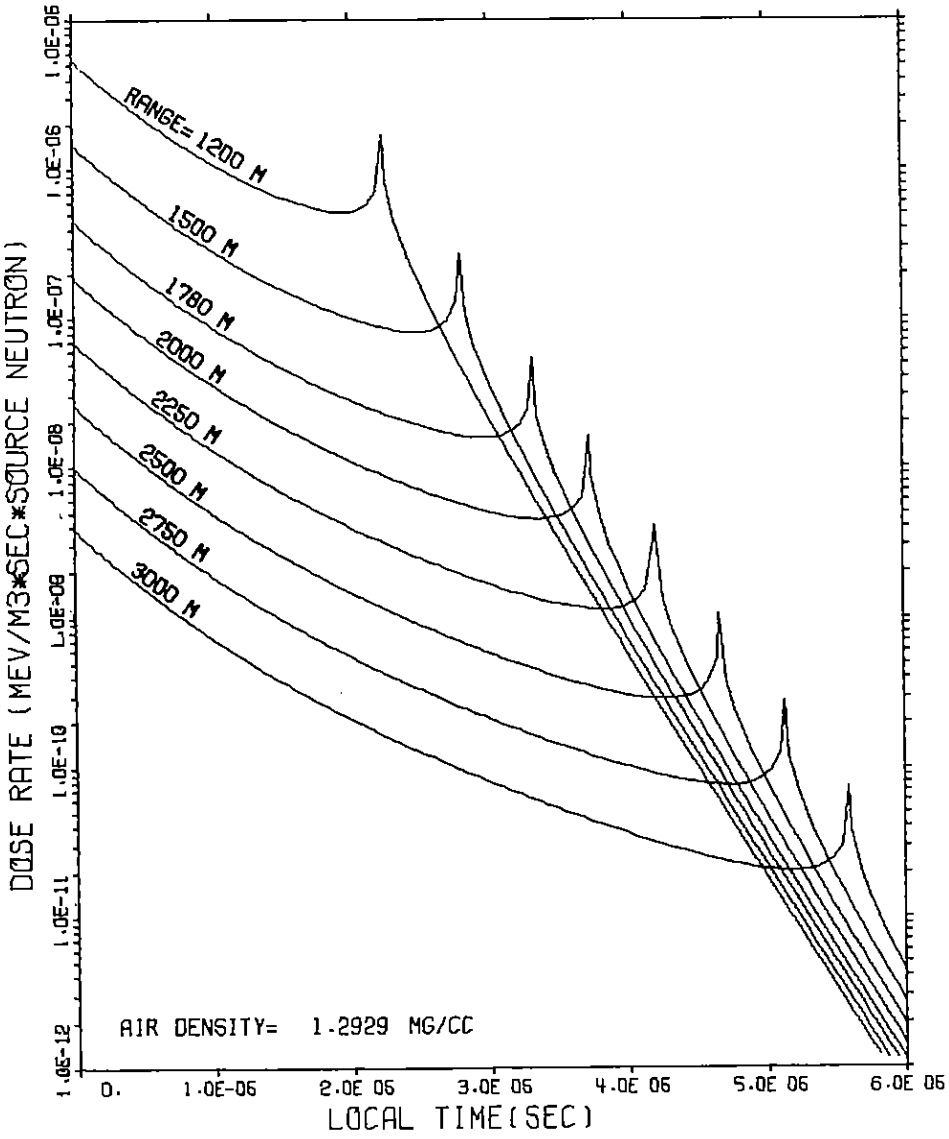

FIG. 14 GAMMA DOSE RATE
NEUTRON SOURCE ENERGY= 10.00 TO 12.20 MEV

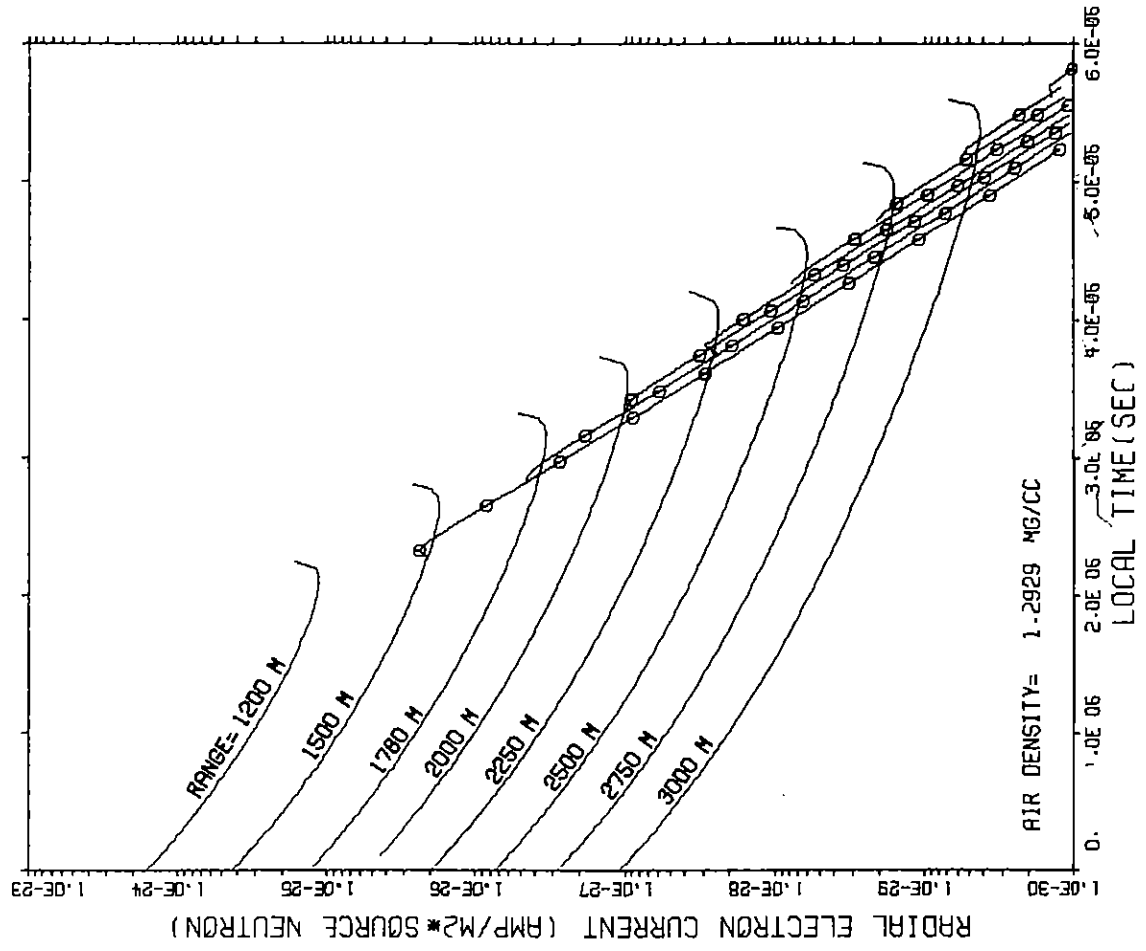

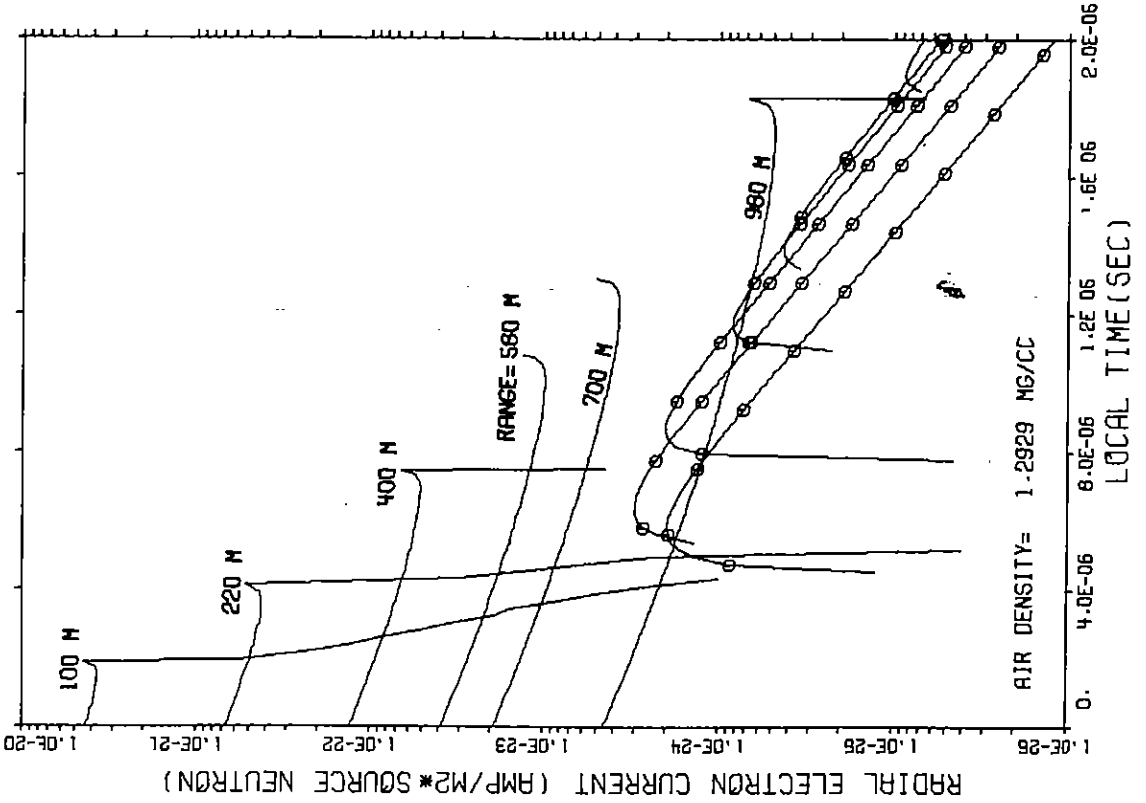

FIG. 15 RADIAL ELECTRON CURRENT
NEUTRON SOURCE ENERGY= 10.00 TO 12.20 MEV

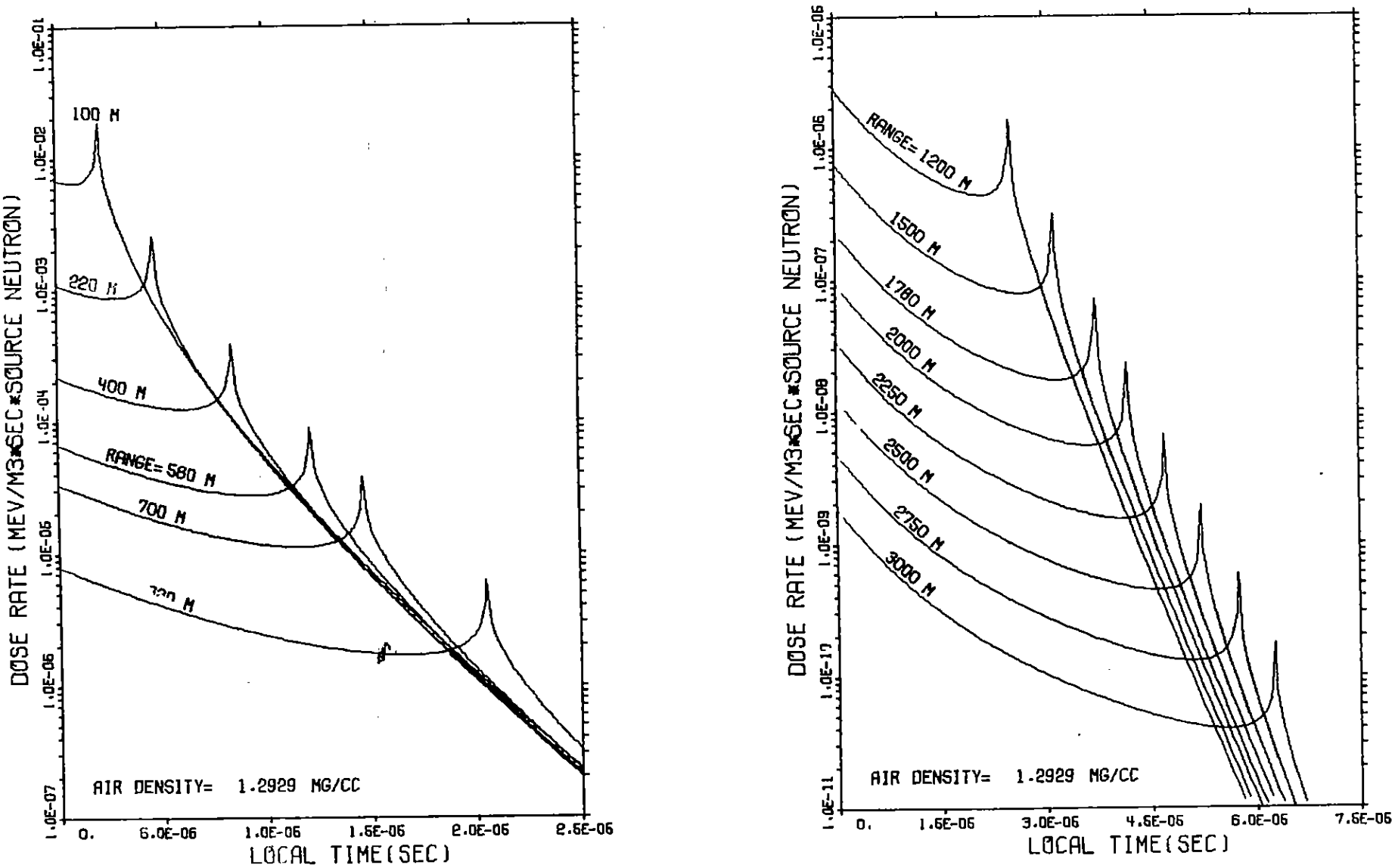

FIG. 16 GAMMA DOSE RATE
NEUTRON SOURCE ENERGY= 8.18 TO 10.00 MEV

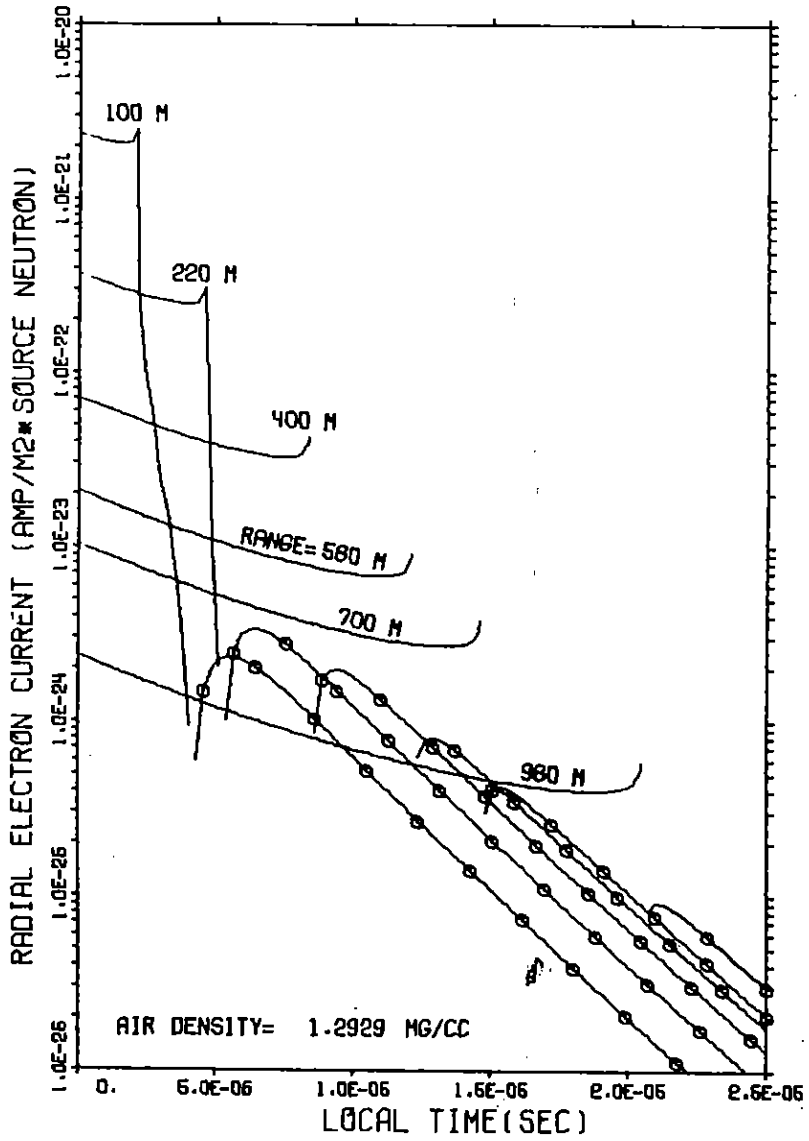

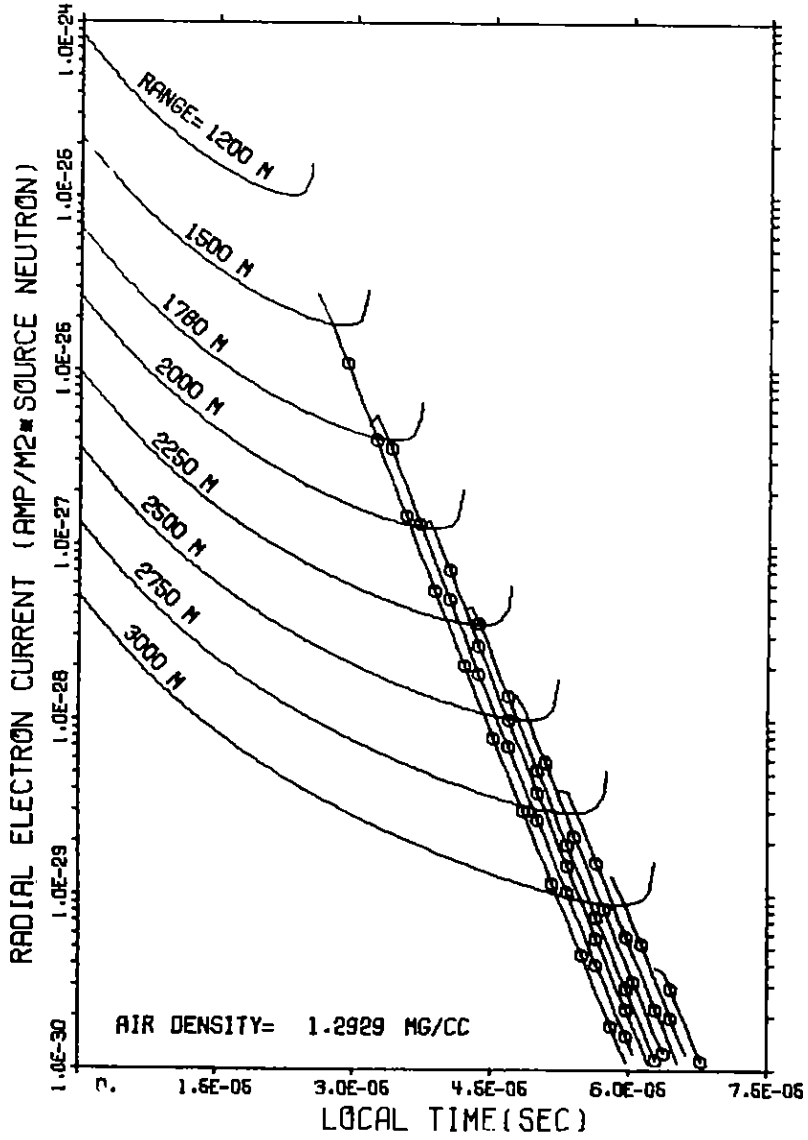

FIG. 17 RADIAL ELECTRON CURRENT
NEUTRON SOURCE ENERGY= 8.18 TO 10.00 MEV

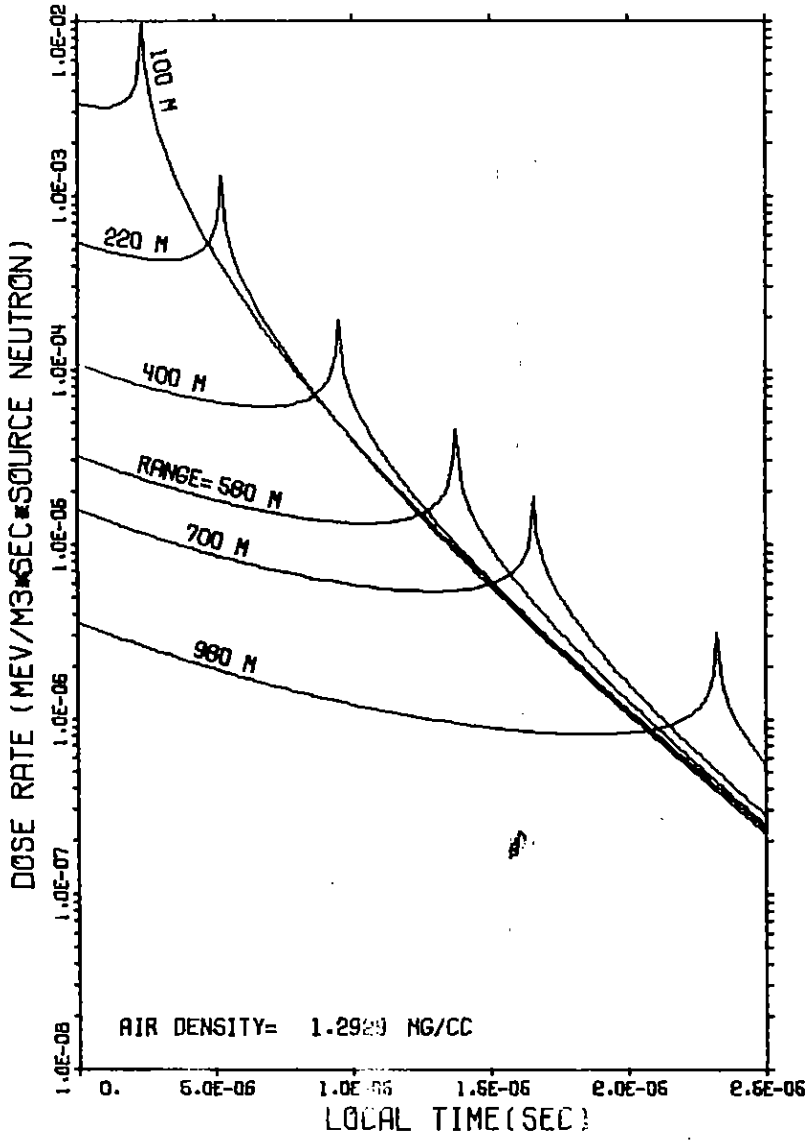

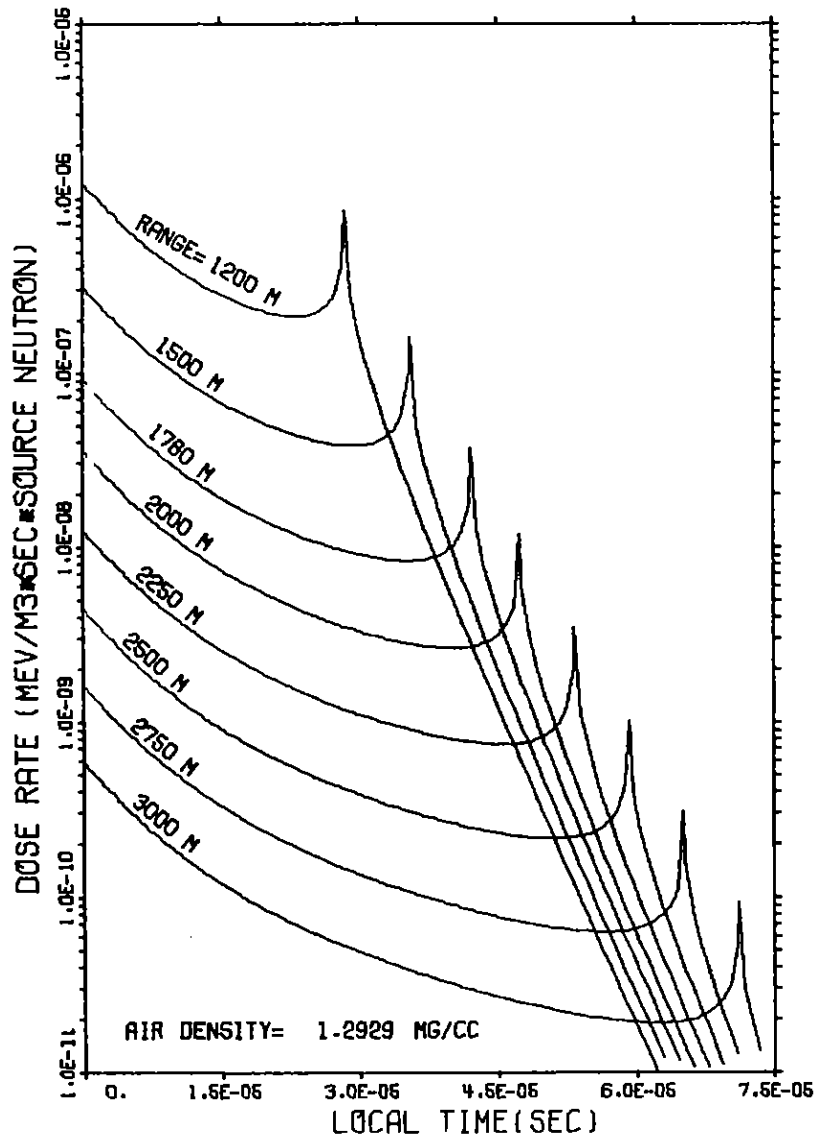

FIG. 18 GAMMA DOSE RATE
NEUTRON SOURCE ENERGY= 6.36 TO 8.18 MEV

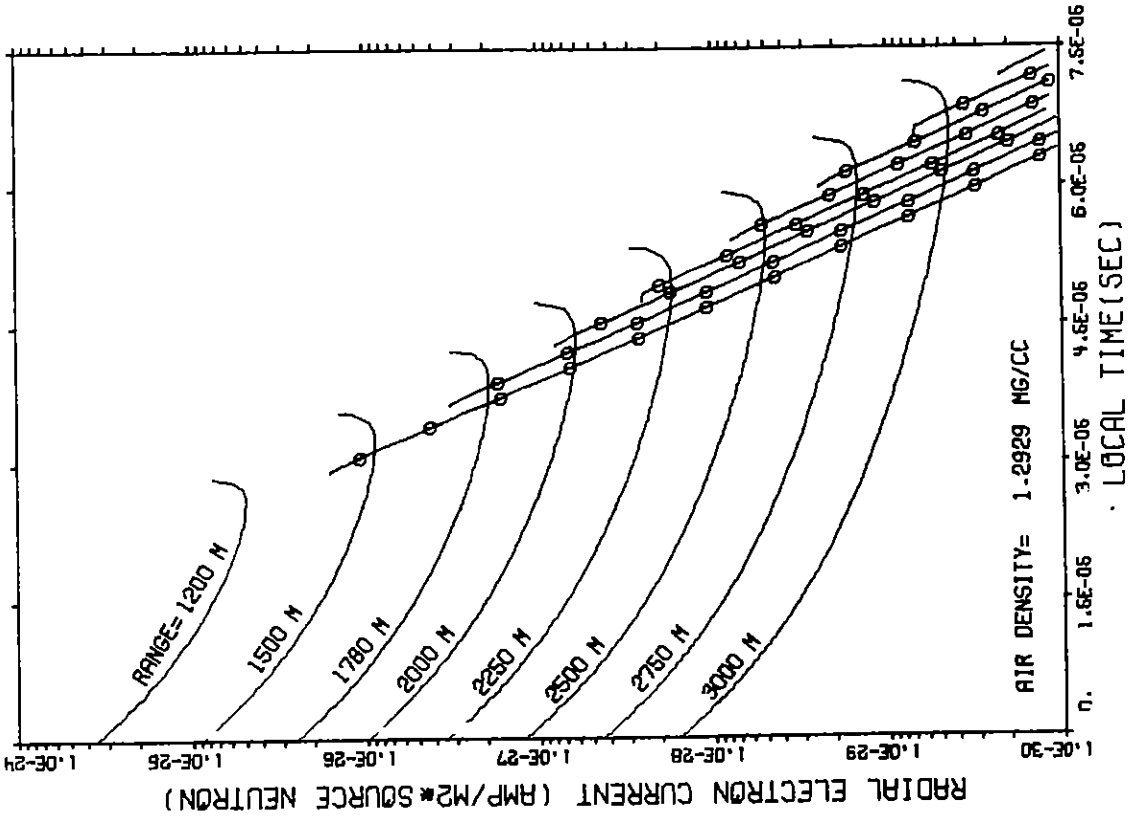

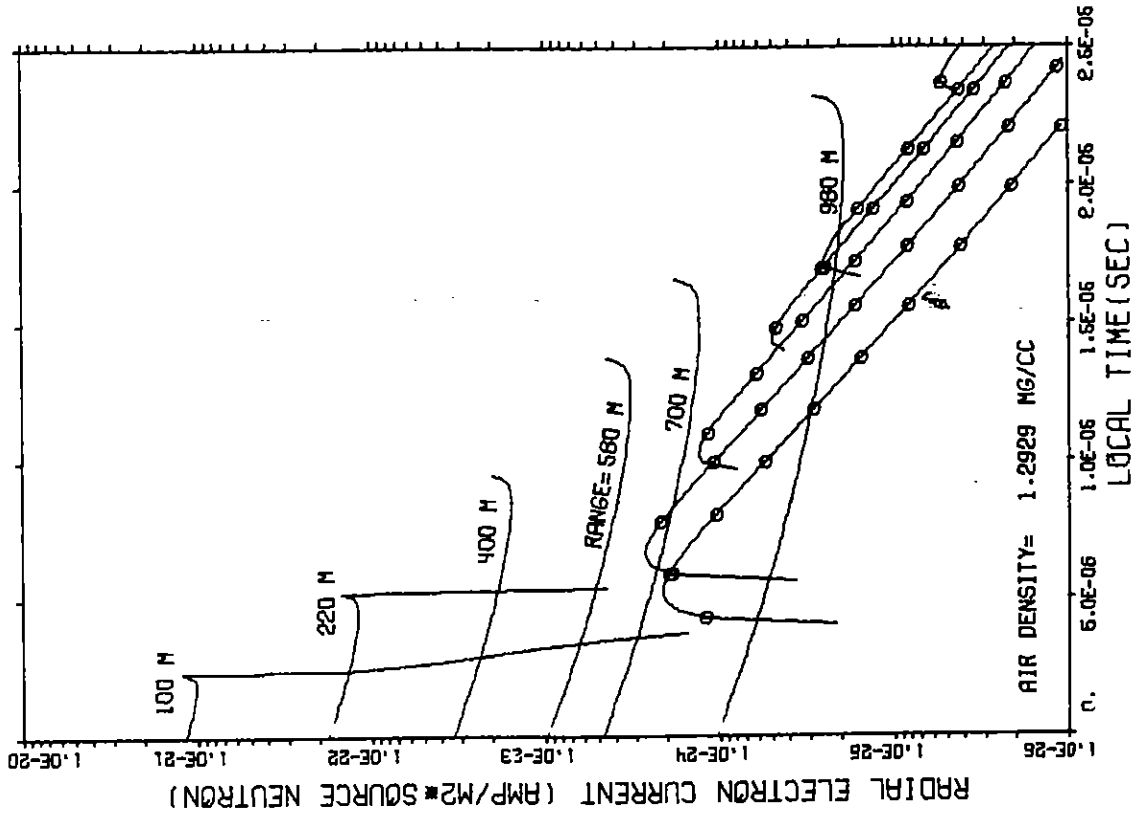

FIG. 19 RADIAL ELECTRON CURRENT
NEUTRON SOURCE ENERGY= 6.36 TO 8.18 MEV

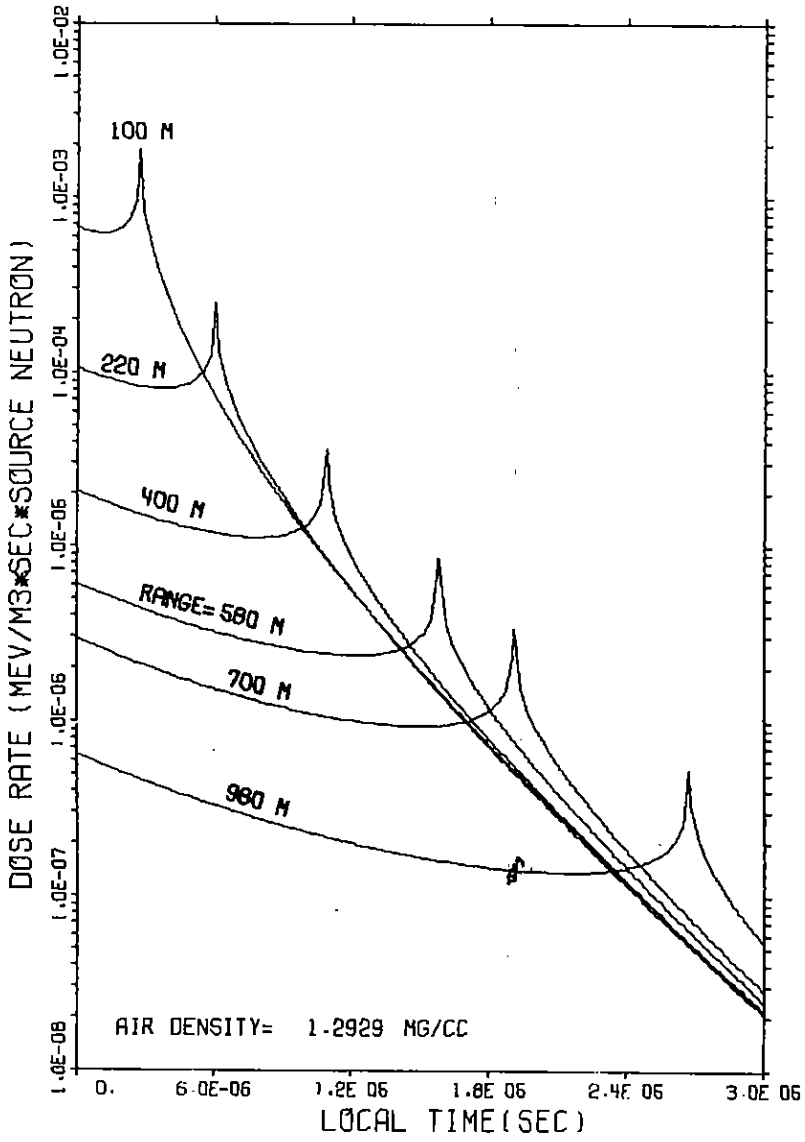

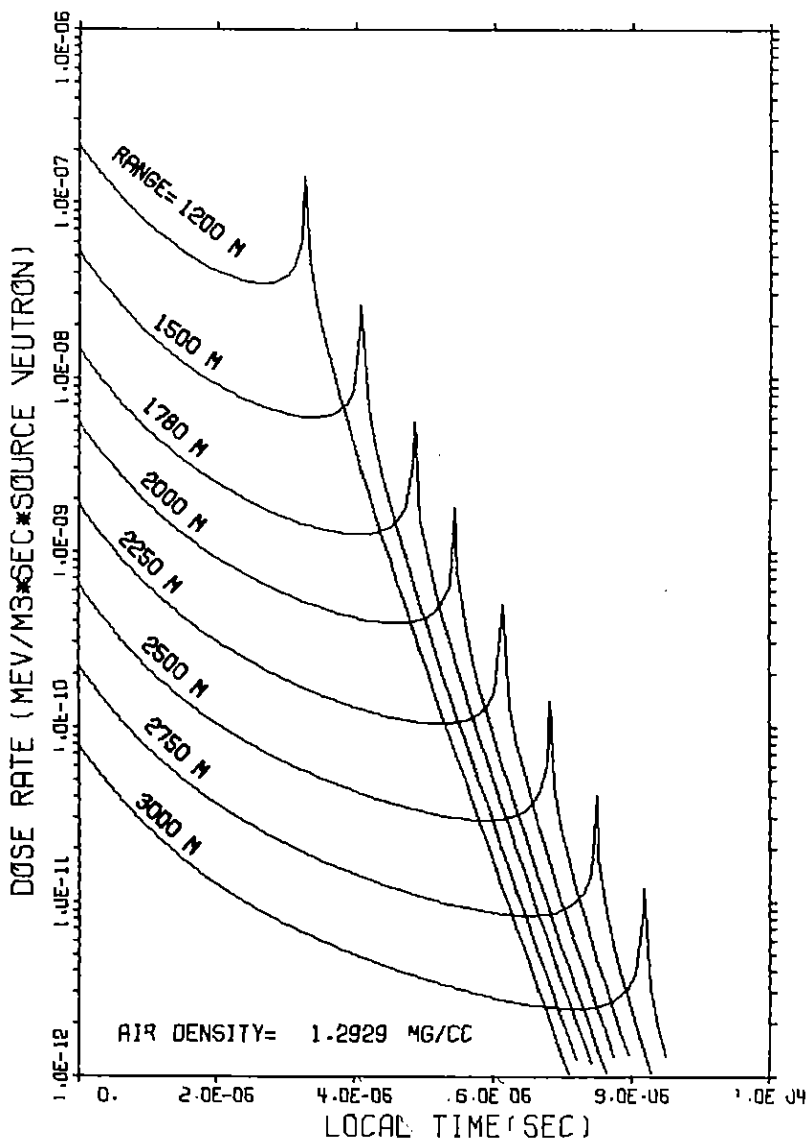

FIG. 20 GAMMA DOSE RATE
NEUTRON SOURCE ENERGY= 4.96 TO 6.36 MEV

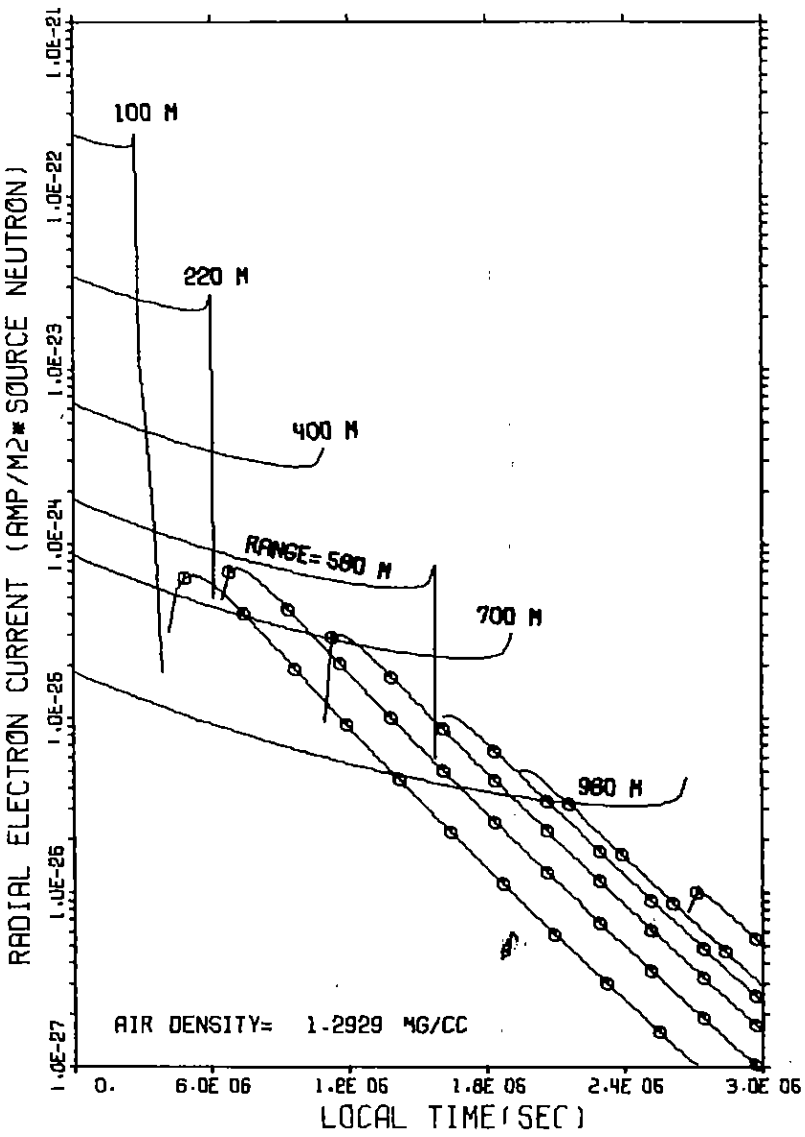

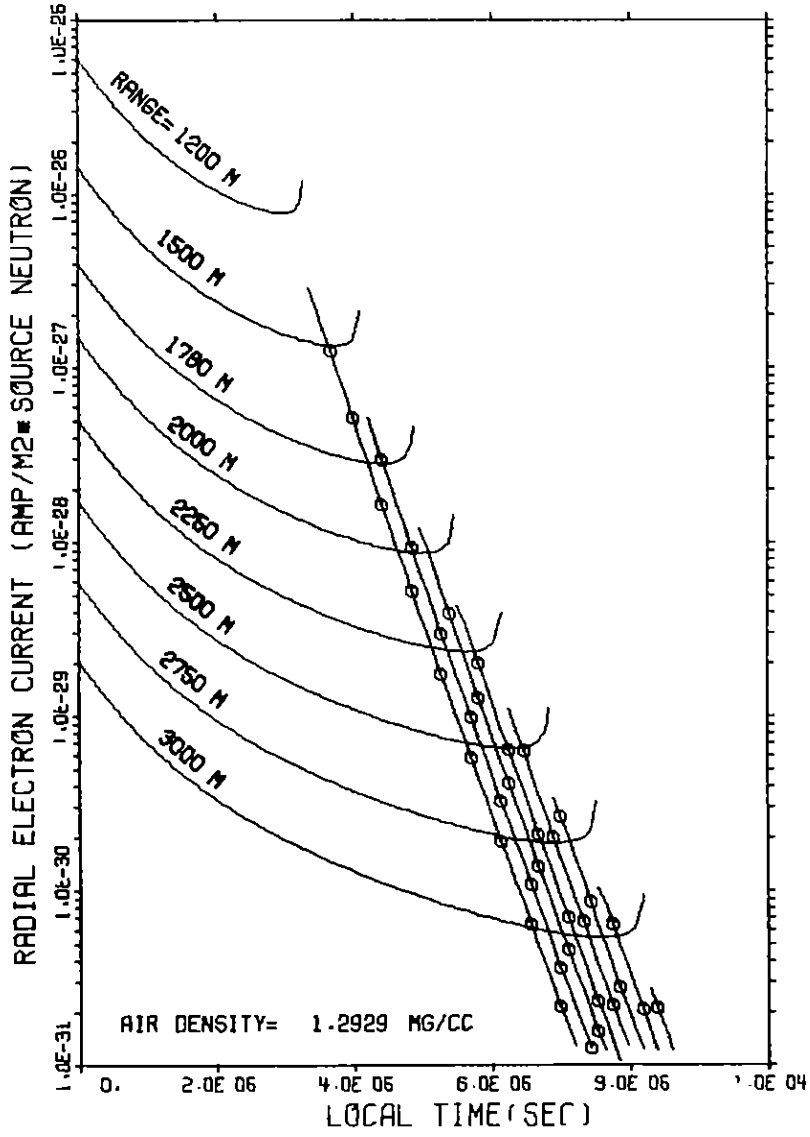

FIG. 21 RADIAL ELECTRON CURRENT
NEUTRON SOURCE ENERGY= 4.96 TO 6.36 MEV

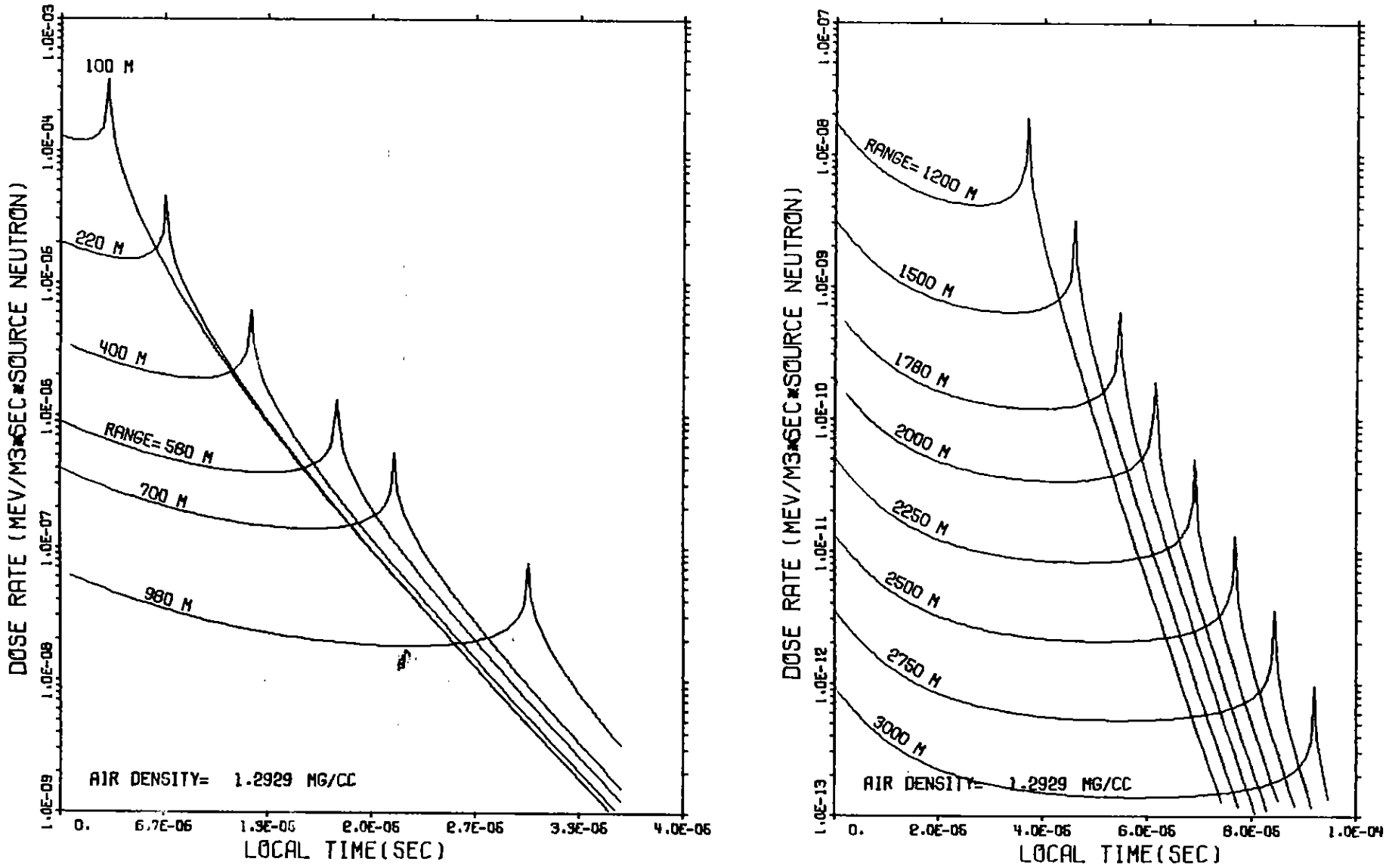

FIG. 22 GAMMA DOSE RATE
NEUTRON SOURCE ENERGY= 4.06 TO 4.96 MEV

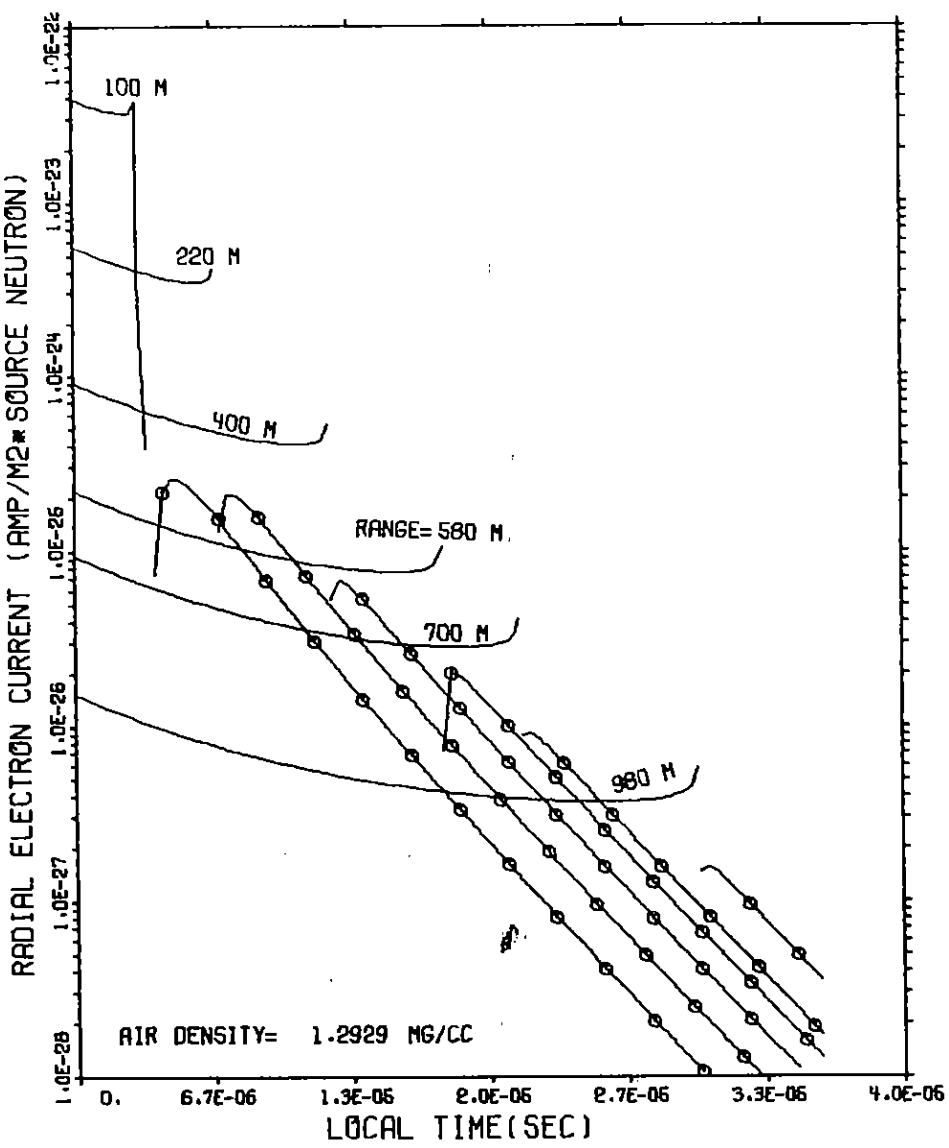

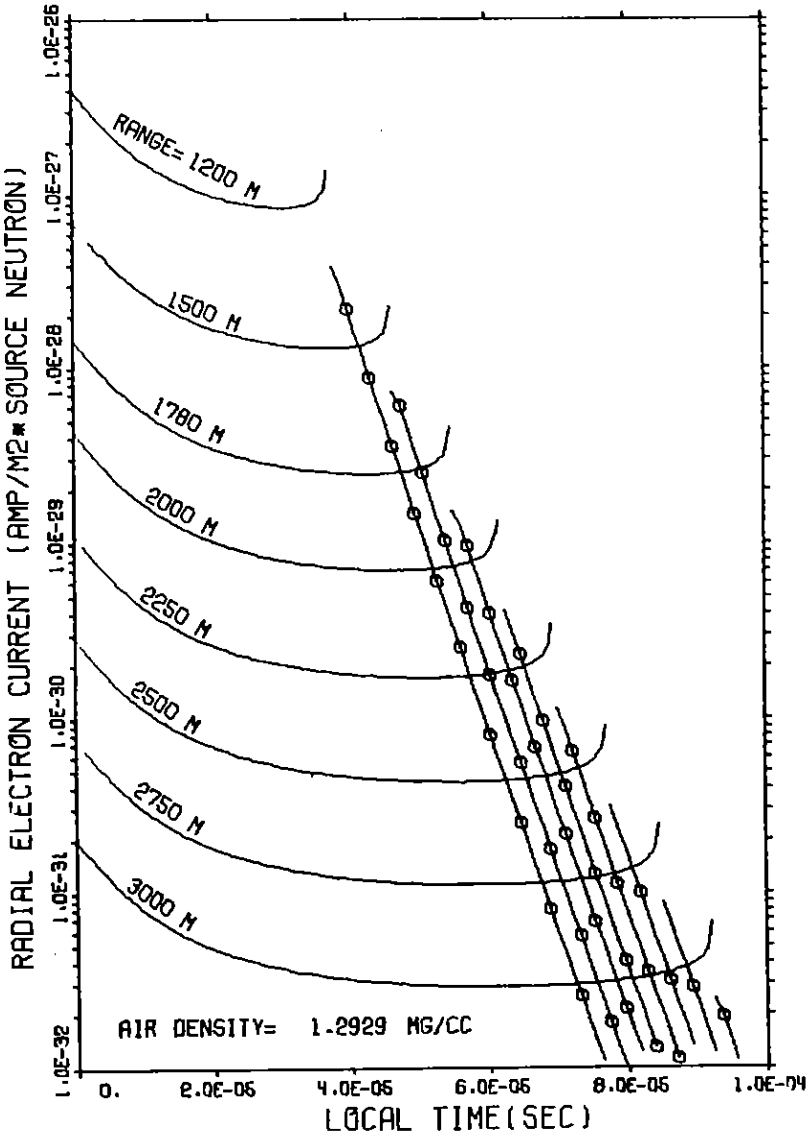

FIG. 23 RADIAL ELECTRON CURRENT
NEUTRON SOURCE ENERGY= 4.06 TO 4.96 MEV

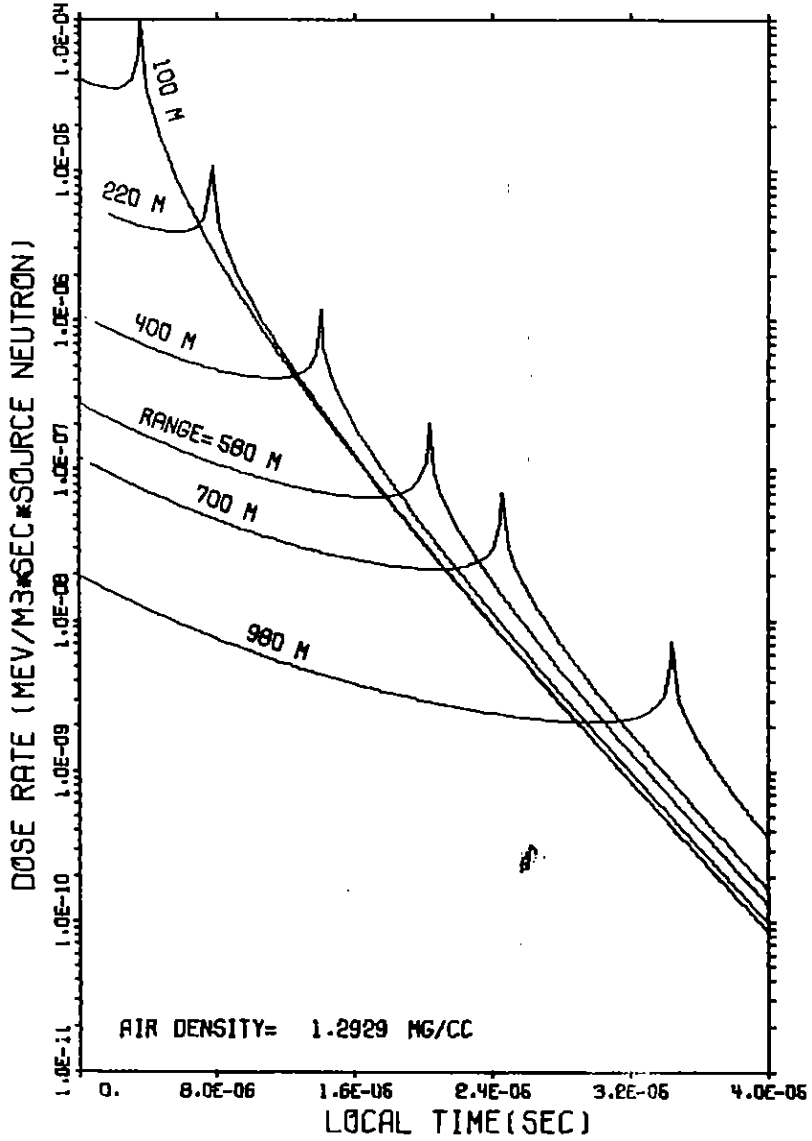

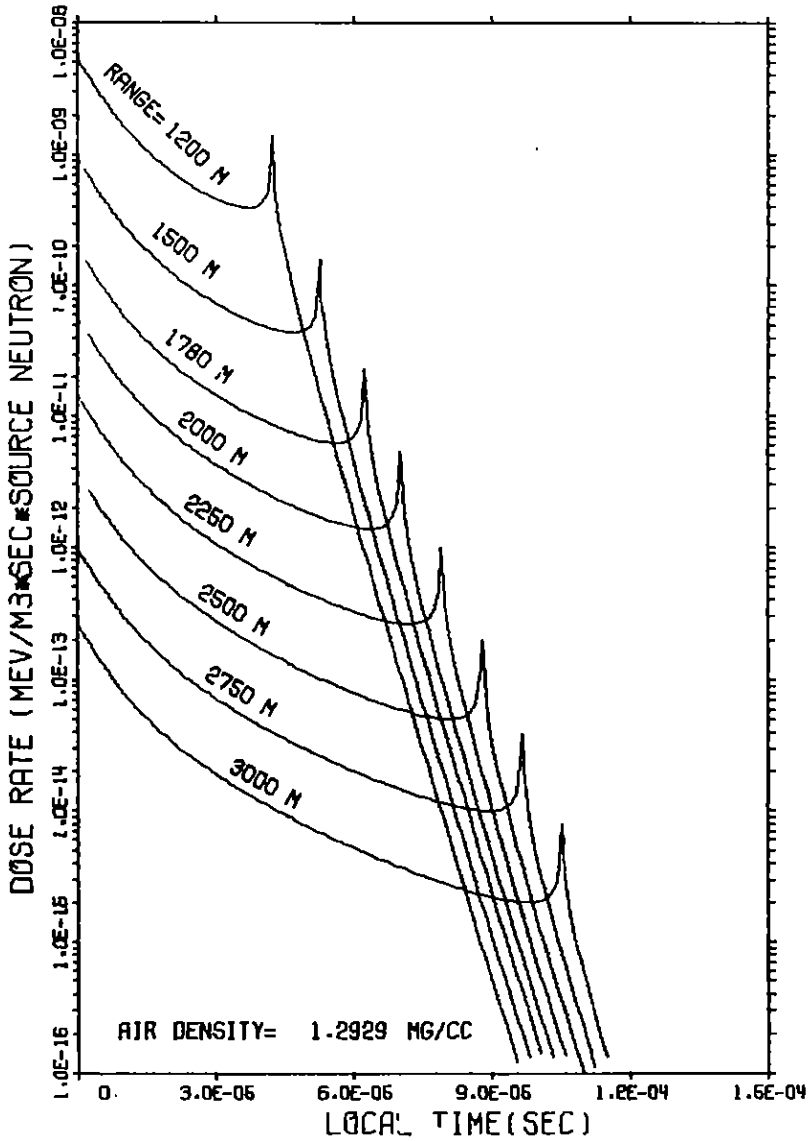

FIG. 24 GAMMA DOSE RATE
NEUTRON SOURCE ENERGY= 3.01 TO 4.06 MEV

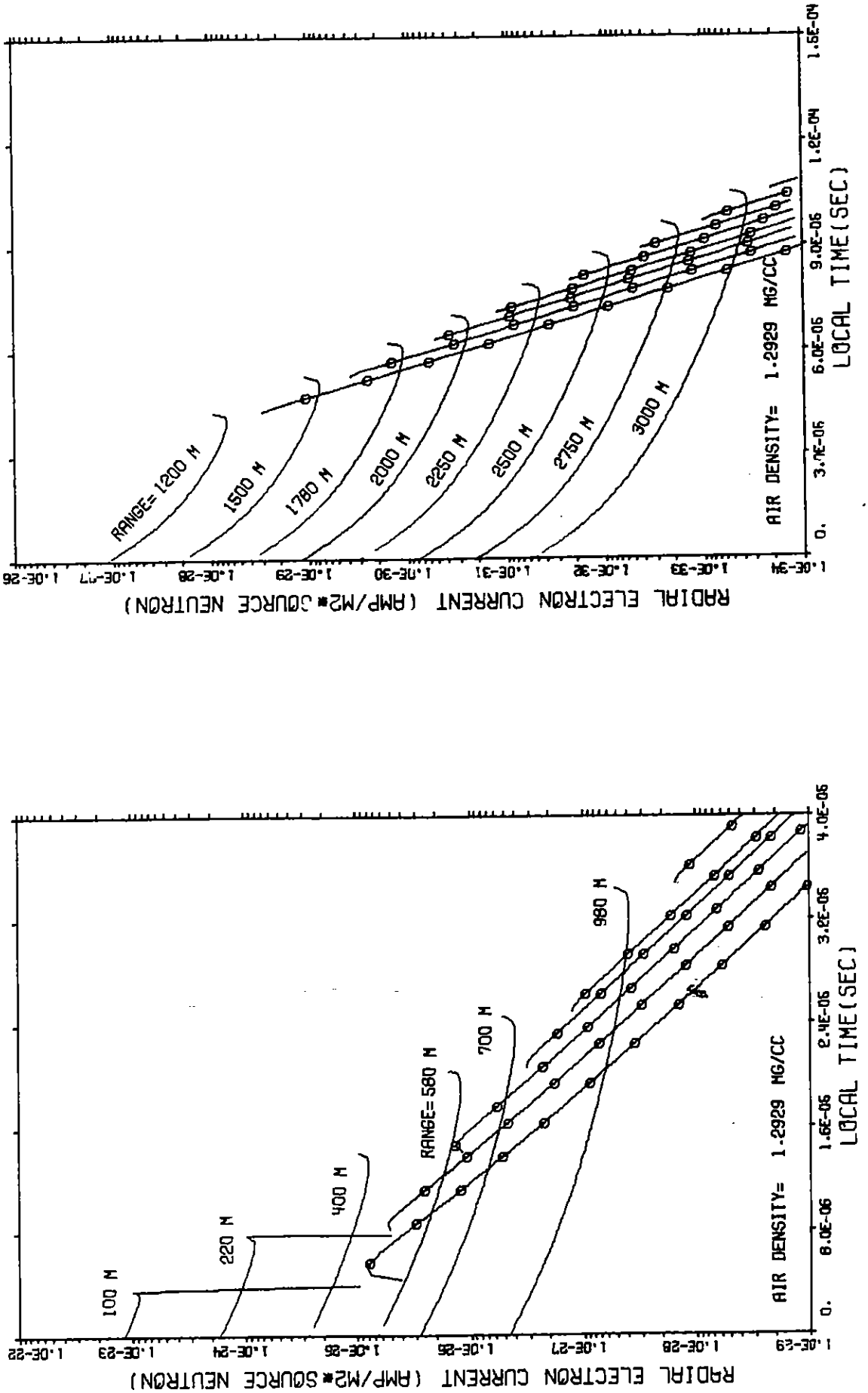

FIG. 25 RADIAL ELECTRON CURRENT
NEUTRON SOURCE ENERGY=3.01 TO 4.06 MEV

APPENDIX

The expressions for dose rate and radial current due to neutron-induced gamma quanta in homogeneous air are obtained, based upon the "shell" model. The underlying assumptions for the extended shell model are listed in the first section, and in the second section expressions for dose rate and radial current are obtained in integral form. These are then rearranged to a closed form in terms of exponential integrals in the third part. Section IV treats the special cases such as, for instance, the solution at the origin. In Section V expressions are developed for dose rate in the case of an exponential build-up factor, and lastly, an extension of the shell model to secondary shells is described in the sixth section.

I. Assumptions for the "Shell" Model

1. A Dirac delta pulse of monoenergetic neutrons is initially emitted from the origin and moves outward as a thin shell at the neutron velocity. To obtain the neutron flux, only absorbing collisions are considered, i.e., scatter is neglected. With these assumptions, the neutron flux from a unit source (one neutron) may be represented:

$$\phi(x,t) = \frac{e^{-\sigma_t x}}{4\pi x^2}\,\delta\left(t-\frac{x}{v}\right) \qquad (1)$$

Where $\phi(x,t)$ = neutron flux
x = distance from origin to shell (see Fig. 1)
t = time from burst
σ_t = attenuation constant (total reaction cross-section)
v = neutron velocity
$\delta(t)$ = Dirac delta function

2. The gamma quanta are emitted isotropically in the laboratory reference system at the point of interaction.

3. The induced gamma quanta are assumed to be monoenergetic in the sense that the energy-dependent parameters are fixed, although these may be average values obtained by averaging over all gamma energies produced.

4. Scattered gammas are accounted for by use of a buildup factor. The buildup factor is in reality a function of time, but it is so rapid compared to the neutron decay time that a good approximation is obtained by assuming an instantaneous buildup. The buildup factors are expressed as functions of the gamma mean free path.

$$D(u) = 1 + b_1 e^{b_2 u} \qquad (2)a$$

$$C(u) = 1 + b_3 e^{b_4 u} \qquad (2)b$$

Where $D(u)$ = steady state dose buildup factor for a point, monoenergetic gamma source

$C(u)$ = steady state radial current buildup factor for a point, monoenergetic gamma source

u = distance from source in mean free paths

b_1, b_2, b_3, b_4 = parameters which depend upon source energy

In developing the formulas for dose rate and radial current, we will omit the exponential from the buildup factor, and then show how it may be incorporated into the final result at the end.*

II. Development of the Expressions for Dose Rate and Radial Current.

The response function which describes the uncollided gamma flux from a point source has a form similar to (1):

$$G(w,t) = \frac{S(t - \frac{w}{c})\, e^{-kw}}{4\pi w^2} \qquad (3)$$

Where $G(w,t)$ = uncollided gamma flux a distance w from the source at time t

$S(t)$ = time dependent gamma source

k = gamma attenuation constant (total reaction cross-section)

c = velocity of light

The gamma source we are interested in is distributed both in space and time, i.e., the expanding shell source indicated in Fig 1. The dose rate and radial current from a ring-shaped differential element of volume may be written:

$$dQ(r,t) = \frac{BUe^{-\sigma_t x}\, \delta(t - x/v - w/c)\, e^{-kw} D(kw)\, 2\pi w^2 dw \sin\theta d\theta}{16\pi^2 x^2 w^2} \qquad (4)$$

* Linear buildup factors are adequate for gamma sources of 3 MEV or greater and for distances less than 7 mean free paths in a water medium, which is similar to air at these energies[7].

$$dJ(r,t) = \frac{BWe^{-\sigma_t x}\ \delta(t-x/v-w/c)e^{-kw}C(kw)dw\cos\theta\sin\theta\, d\theta}{8\pi x^2} \qquad (5)$$

Where $dQ(r,t)$ = dose rate at position r, time t due to ring source at x

$dJ(r,t)$ = component of electron current in the radial direction due to ring source at x.

B = gamma production cross-section

U = flux-to-dose conversion factor

W = gamma current to radial current conversion factor

The use of conversion factors is valid as the deposition of ionizing energy by Compton recoil electrons, pair production, and photoelectric effect may be considered local processes. This follows from the high ratio of gamma mean free path to electron range which is of the order 100.

$$U = \sum_{i=1}^{3} \sigma_{di} E_i \qquad (6)a$$

$$W = -\frac{eR}{\lambda_c} \qquad (6)b$$

Where σ_{di} = cross section for i^{th} ionizing reaction

E_i = average ionizing energy deposited in the i^{th} reaction

e = electronic charge

R = average range of recoil electron in direction of incident gamma

λ_c = gamma mean free path for compton collision

We choose to do the spatial integrations of (4) and (5) in a coordinate system centered at the observer position rather than at the burst point, and eliminate the angle variable θ by utilizing the following property of the Dirac delta function.

$$\int \delta[y(s)]f(s)ds = \left|\frac{f(s_o)}{\frac{dy}{ds}}\right|_{y=0} \qquad (7)$$

Where s_o satisfies $y(s_o) = 0$

Let $y = t - x/v - w/c$ (8)a

$s = \cos\theta$ (8)b

Application of the law of cosines to the triangle bounded by x, w, and r of Fig. 1 yields

$$x^2 = r^2 + w^2 - 2rw\cos\theta \tag{9}$$

If x is eliminated from (8)a and (9), and the derivative indicated in (7) is taken, the result is:

$$\left.\frac{dy}{ds}\right|_{y=o} = \frac{crw}{v^2(ct-w)} \tag{10}$$

$$x = \frac{v}{c}(ct-w) \tag{11}$$

Now we may apply (7) to (4) and (5), integrating over θ to obtain

$$Q(r,t) = \int_{w1}^{w2}\int_{o}^{\pi} dQ(r,t) = \int_{w1}^{w2} \frac{BUce^{-at}\, e^{\frac{-w\Delta\nu}{c}}\, D(kw)\,dw}{8\pi rw(ct-w)} \tag{12}$$

$$J(r,t) = \int_{w1}^{w2}\int_{o}^{\pi} dJ(r,t) = \int_{w1}^{w2} \frac{BWce^{-at}\, e^{\frac{-w\Delta\nu}{c}}\, [r^2+w^2-(ct-w)^2/\xi^2]\, C(kw)\,dw}{16\pi r^2w^2(ct-w)} \tag{13}$$

Where $a = \sigma_t v$ = neutron collision frequency

$\nu = kc$ = gamma collision frequency

$\Delta\nu = \nu - a$ (14)

$\xi = c/v$

$\eta = r/vt$

The next task is to determine the limits of integration w1 and w2. Recall equation (9) from the law of cosines.

$$x^2 = r^2 + w^2 - 2rw \cos\theta \tag{9}$$

The maximum and minimum values of w must occur at $\cos\theta = \pm 1$, and at the same time satisfy (11).

$$x = \frac{v}{c}(ct-w) \tag{11}$$

The solution is listed below.

$$w1 = \begin{cases} \dfrac{vt-r}{1+1/\xi} & r < vt \\ \dfrac{r-vt}{1-1/\xi} & r > vt \end{cases} \tag{15a}$$

$$w2 = \frac{vt+r}{1+1/\xi} \tag{15b}$$

Having obtained expressions (12) and (13) for dose rate and radial current, along with expressions (15)a and (15)b for the limits of integration, we could end the development of the extended shell model at this point and obtain results by a numerical integration. In addition, no special use has been made of the form of the buildup factor expressions, so at this point these may be arbitrary functions.

III. Solutions in Terms of Exponential Integrals.

It is possible to obtain the solutions in a closed form by expressing them as products of exponentials and exponential integrals. A very useful byproduct of doing this is that special limiting cases may be easily treated by making use of the properties of exponential integrals. The two exponential integrals of interest are defined as follows:[8]

$$E1(z) = \int_z^\infty \frac{e^{-u}}{u}\,du \tag{16a}$$

$$EI(z) = \int_{-\infty}^{z} \frac{e^u}{u}\,du \quad \text{(principle value)} \tag{16)b}$$

To proceed, we expand the integrands of (12) and (13), defined respectively Q1 and J1, by partial fractions.

$$Q1 = A1e^{\frac{-w\Delta\nu}{c}}\left(\frac{A_2}{w} + \frac{A_3}{ct-w}\right) \tag{17}$$

$$J1 = A4e^{-at}e^{\frac{-w\Delta\nu}{c}}\left(A_5 + \frac{A_6}{w} + \frac{A_7}{w^2} + \frac{A_8}{ct-w}\right) \tag{18}$$

Where $A1 = \dfrac{BUe^{-ft}}{8\pi rt}$ (19)a

$A2 = 1$ (19)b

$A3 = 1 + \nu t b_1$ (19)c

$A4 = \dfrac{WB\nu}{16\pi r^2\xi}$ (19)d

$A5 = \nu b_1 (1-\xi^2)/c$ (19)e

$A6 = \eta^2 + 1 + \nu t b_1 (\eta^2-1)$ (19)f

$A7 = ct(\eta^2 - 1)$ (19)g

$A8 = (\eta^2 + \xi^2)(1 + \nu t b_1)$ (19)h

The following integrals will also be required in completing the development.

$$\int \frac{e^{\frac{-w\Delta\nu}{c}}}{w^2}\,dw = -\frac{e^{\frac{-w\Delta\nu}{c}}}{w} - \frac{\Delta\nu}{c}\int \frac{e^{\frac{-w\Delta\nu}{c}}}{w}\,dw \tag{20}$$

$$\int_{w1}^{w2} \frac{e^{\frac{-w\Delta\nu}{c}}}{w}\,dw = \int_{\frac{\Delta\nu w1}{c}}^{\frac{\Delta\nu w2}{c}} \frac{e^{-u}}{u}\,du \tag{21}$$

$$\int_{w1}^{w2} \frac{e^{\frac{-w\Delta\nu}{c}}}{ct-w}\,dw = e^{-\Delta\nu t}\int_{\frac{\Delta\nu}{c}(ct-w2)}^{\frac{\Delta\nu}{c}(ct-w1)} \frac{e^{u}}{u}\,du \tag{22}$$

Note that (21) and (22) may be written as the difference of two exponential integrals. Utilizing equations (17) through (22) we may now perform the integration over w.

$$Q(r,t) = \int_{w1}^{w2} Q1\,dw$$

$$= \frac{BU}{8\pi rt}\left[e^{-at}\int_{\frac{\Delta\nu}{c}w1}^{\frac{\nabla\nu}{c}w2} \frac{e^{-u}}{u}\,du + (1+\nu tbl)e^{-\nu t}\int_{\frac{\Delta\nu}{c}(ct-w2)}^{\frac{\Delta v}{c}(ct-w1)} \frac{e^{u}}{u}\,du \right] \tag{23}$$

$$J(r,t) = \int_{w1}^{w2} J1\,dw$$

$$= A4\left\{ e^{-ft}\left[e^{-\frac{\Delta\nu w1}{c}}\left(\frac{cA5}{\Delta\nu} + \frac{A7}{w1}\right) - e^{\frac{-\Delta\nu w2}{c}}\left(\frac{cA5}{\Delta\nu} + \frac{A7}{w2}\right) \right.\right.$$

$$\left.\left. + \left(A6 - \frac{\Delta\nu A7}{c}\right)\int_{\frac{\Delta\nu w1}{c}}^{\frac{\Delta\nu w2}{c}} \frac{e^{-u}}{u}\,du \right] + A8e^{-\nu t}\int_{\frac{\Delta\nu}{c}(ct-w2)}^{\frac{\Delta\nu}{c}(ct-w1)} \frac{e^{u}}{u}\,du \right\} \tag{24}$$

Before writing out the results in full, we define the following values in order to make the result less bulky.

$$z1 = \begin{cases} \Delta\nu\left(\frac{vt-r}{c+v}\right) & r < vt \\ \Delta\nu\left(\frac{r-vt}{c-v}\right) & r > vt \end{cases} \qquad (25)a$$

$$z2 = \Delta\nu\left(\frac{vt + r}{c + v}\right) \qquad (25)b$$

$$z3 = \begin{cases} \Delta\nu\left(\frac{ct + r}{c + v}\right) & r < vt \\ \Delta\nu\left(\frac{ct - r}{c - v}\right) & r > vt \end{cases} \qquad (25)c$$

$$z4 = \Delta\nu\left(\frac{ct - r}{c+v}\right) \qquad (25)d$$

$$Q(r,t) = \frac{BU}{8\pi rt}\left\{ e^{-at}[El(z1)-El(z2)] + (1+\nu tbl)e^{-\nu t}[EI(z3)-EI(z4)] \right\} \qquad (26)$$

$$J(r,t) = \frac{BW\nu}{16\, r^2\xi}\left\{ e^{-at}\left[e^{-z1}\left(\frac{\nu b3(1-\xi^2)}{\Delta\nu} + \frac{\Delta\nu t(\eta^2-1)}{z1}\right)\right.\right.$$

$$-e^{-z2}\left(\frac{\nu b_3(1-\xi^2)}{\Delta\nu} + \frac{\Delta\nu t(\eta^2-1)}{z2}\right)$$

$$\left.\left. + (\eta^2 + 1 + t\,(\nu b_3 - \Delta\nu)(\eta^2-1))(El(z1)-El(z2))\right]\right.$$

$$\left. + (\eta^2 + \xi^2)(1 + \nu t b_3)e^{-\nu t}\,[EI(z3) - EI(z4)]\right\} \qquad (27)$$

IV. Special Cases

To be complete, there are several special cases which must be handled separately. The expressions for these special cases are simply stated to avoid lengthy developments.

1. $\Delta\nu < 0$, or $f > \nu$

Replace [El(z1) - El(z2)] by [EI(z2) - EI(z1)] and replace[EI(z3) - EI(z4)] by [El(z4) - El(z3)] in equations (26) and (27).

2. $\Delta\nu = 0$, or $a = \nu$

$$Q(r,t) = \frac{BU}{8\pi rt}\, e^{-at} \begin{cases} \ln\left(\frac{vt+r}{vt-r}\,\frac{ct+r}{ct-r}\right) + \nu t b_1 \ln\left(\frac{ct+r}{ct-r}\right) & r < vt \\ \ln\left(\frac{r+vt}{r-vt}\right) + \nu t b_1 \ln\left(\frac{c+v}{c-v}\right) & r > vt \end{cases} \qquad (28a)$$

$$J(r,t) = \frac{BUv}{16\pi r^2\xi}\, e^{-at} \left\{ -2\eta\,[1 + \xi + \nu t b_3(\xi-1)]\right.$$

$$+ [\eta^2 + 1 + \nu t b_3(\eta^2-1) \ln\left(\frac{vt+r}{vt-r}\right) \qquad (29a)$$

$$\left. + (1 + \nu t b_3)(\eta^2+\xi^2) \ln\left(\frac{ct+r}{ct-r}\right)\right\} \qquad r < vt$$

$$J(r,t) = \frac{BWv}{16\pi r^2\xi}\, e^{-at} \left\{ 2(\xi-\eta)(1-\nu t b_3)\right. \qquad (29b)$$

$$+ [\eta^2 + 1 + \nu t b_3(\eta^2-1)] \ln\left(\frac{r+vt}{r-vt}\,\frac{c-v}{c+v}\right)$$

$$\left. + (1 + \nu t b_3)(\eta^2 + \xi^2) \ln\left(\frac{c+v}{c-v}\right)\right\} \qquad r > vt$$

3. $r = 0$

$$Q(0,t) = \frac{BU(c+v)}{4\pi(vt)^2\,\xi}\left(1+\frac{vt\nu b_1}{v+c}\right)\exp\left(-\frac{ct(\sigma_t+k)}{1+\xi}\right) \qquad (30)a$$

$$J(0,t) = 0$$

4. $r = ct$

$$Q(ct,t) = \frac{BU}{8\pi ct^2}\,(1+\nu t b_1)\,e^{-\nu t}\,\ln\left(\frac{c+v}{c-v}\right) \qquad (31)a$$

$$J(ct,t) = \frac{BW}{8\pi ct^2}\,(1+\nu t b_3)\,e^{-\nu t}\,\ln\left(\frac{c+v}{c-v}\right) \qquad (31)b$$

It should be noted here that in reality there is no buildup of dose rate or current at the arrival time of the gamma wave, and the buildup factors appear here because of the assumption of instantaneous buildup.

5. $r = vt$

The treatment of this case is approximate and therefore requires a more detailed explanation. For a delta function source, there is a logarithmic singularity at the neutron arrival time, $t = r/v$. However, real sources are never delta functions in time, so we arbitrarily remove the singularity by assuming a square source pulse of duration Δt and magnitude $1/\Delta t$, where Δt is approximately the duration of the real source.

To proceed, we note that only terms involving z1 in equations (26) and (27) are giving trouble. If t is sufficiently small, the value of Q and J at $t = r/v$ can be obtained by approximating the troublesome terms by average values, and evaluating all other terms in the normal way. That is, over the range $r/v - \Delta t/2 \leq t \leq r/v + \Delta t/2$ all but the troublesome terms are assumed to be constant. The exponential integral expanded to terms of first order in its argument may be written:[8]

$$E1(x) \cong -\Gamma - \ell n\, x + x \qquad (32)$$

Using this expansion in the following integral, we obtain the approximate average value.

$$\overline{El} = \frac{2}{\Delta t}\int_{To-\frac{\Delta t}{2}}^{To} El\left(\Delta\nu\,\frac{r-vt}{c-v}\right)dt + \frac{2}{\Delta t}\int_{To}^{To+\frac{\Delta t}{2}} El\left(\Delta\nu\,\frac{vt-r}{c+v}\right)dt$$

$$\tilde{=}\ 1 - \gamma - \frac{1}{2}\ln\left(\frac{(\Delta\nu v\Delta t)^2}{4(c^2-v^2)}\right) \qquad (33)a$$

Where $To = r/v$

$\gamma = .5772157$

Let $Z = \frac{\Delta\nu t(\eta^2-1)}{z1}$ (34)

An average value for Z must be found since Z has a different limiting value at $t = To$ for $t > To$ and $t < To$. This average value is simply taken to be the arithmetic mean of the two limiting values.

$$\overline{Z} = \frac{1}{2}\ [(1+\eta)(1+\xi) - (1+\eta)(\xi-1)$$

$$\overline{Z} = 2\,\frac{(1+\eta)}{2} = 2 \qquad (35)a$$

It was found after applying these expressions that the discontinuity in Z had a greater effect on the radial current than the logarithmic term for a value of $\Delta t = 2 \times 10^{-8}$ sec. The manifestation of this was an abrupt decrease in current at arrival time rather than a peak. It turns out, however, that a peak value of current does occur if the average values are computed entirely before arrival time. Thus, let

$$\overline{El'} = \frac{1}{\Delta t}\int_{To-\Delta t}^{To} El\left(\Delta\nu\,\frac{r-vt}{c-v}\right)dt$$

$$= 1 - \gamma - \ln\frac{\Delta\nu v\Delta t}{c-v} \qquad (33)b$$

$$\overline{Z'} = -(1+\eta)(\xi-1) = -2(\xi-1) \qquad (35)b$$

Now Q may be evaluated at the singularity by replacing El(z1) in equation (26) by $\overline{El}$ (equation (33)a), and J may be evaluated by replacing El(z1) and Z in equation (27) by $\overline{El'}$ and $\overline{Z'}$ as indicated in (33)b and (35)b, evaluating all other terms in the normal way, setting $t = To$.

6. Exponential buildup factor.

Lastly, if $b_2 \neq 0$ in (2)a, the expression for dose buildup factor, we indicate the correction that must be made to equation (26).

$$Q(r,t) = \frac{BU}{8\pi rt} \left\{ e^{-at} [E1(z1) - E1(z2)] \right.$$

$$+ e^{-\nu t} [EI(z3) - EI(z4)]$$

$$\left. + \nu t b_1 e^{-\nu' t} [EI(z'3) - EI(z'4)] \right\} \qquad (35)$$

Where $\nu' = kc\,(1 - b_2)$ (36)a

$$\Delta\nu' = \nu' - f$$

$$z3' = \begin{cases} \Delta\nu' \left(\frac{ct+r}{c+v} \right) & r < vt \\ \Delta\nu' \left(\frac{ct-r}{c-v} \right) & r > vt \end{cases} \qquad (36)b$$

$$z4' = \Delta\nu' \left(\frac{ct-r}{c+v} \right) \qquad (36)c$$

Equation (27) for radial current is modified in a similar fashion if $b_4 \neq 0$ in the expression for radial current buildup factor.

VI. Extension of the Shell Model.

A possible extension of the shell model may be mentioned here. It is possible to arbitrarily "create" a secondary source shell; for instance, such a secondary shell might be used to represent the neutrons elastically scattered from the uncollided neutron shell. These elastically scattered neutrons continue to possess a relatively high energy. The existing number of these secondary neutrons at any given time may be represented by a sum of exponentials[6]. To illustrate the technique, let it be assumed that a secondary shell of neutrons is travelling out from the origin, and its spatially integrated value is a single exponential,

$$pe^{-a_2 t/v'},$$

where p is a constant and v' is the radial velocity of the shell. The geometry is the same as that of fig. 1. The gamma source from an element of this shell would be represented

$$S(x,t) = \frac{pBe^{-a_2 t}}{4\pi x^2} \xi(t - x/v') \; d\,(vol) \; . \qquad (37)$$

The uncollided gamma flux from an element of the shell would then be

$$G(w,t) = \frac{pBe^{-a_2(t-w/c)} \delta(t-w/v'-w/c) e^{-kw} \, d(vol)}{16\pi^2 w^2 x^2} \qquad (38)$$

Further steps in the development will not affect the exponential exp $(-a_2 t)$ since t is held fixed. Thus, if the expressions previously derived for dose rate and radial current are multiplied by p, a is replaced by a_2, k is replaced by $k - a_2/c$, and the appropriate B for gamma production is used, the same expressions may be used to estimate the dose rate and radial current from gamma quanta produced by the interactions of elastically scattered neutrons in a "secondary shell".

References

1. R. R. Schaefer, "Charge Currents and Conductivity Arising from Inelastic and Fast Captance Collisions of Neutrons in Air Surrounding a Nuclear Detonation," Electromagnetic Pulse Theoretical Note XV, (1966).
2. D.A. Moody, "The Compton Currents and Ionization Rate Generated in a Non-Uniform Atmosphere by Fast, Mono-Energetic Neutrons from a Point Source," AWRE-0-13/67, (1967).
3. R.E. LeLevier, "The Compton Current and the Energy Deposition Rate from Gamma Quanta - A Monte Carlo Calculation," RM-4151-PR, Rand Corporation, (1964). Also Electromagnetic Pulse Theoretical Note XXXVII.
4. M.D. Goldberg, et al., "Angular Distributions in Neutron-Induced Reactions Volume I, Z=1,22," BNL-400 Second Edition, Volume I, Brookhaven National Laboratory (October 1962).
5. H.C. Honeck, "ENDF/B, Specifications for an Evaluated Nuclear Data File for Reactor Applications," BNL-50066.
6. C.R. Hale, "Radial Current and Dose Rate from Neutron Induced Gamma Quanta in Uniform Air by Means of the Stationary Source Approximation," Electromagnetic Pulse Theoretical Note 63, (1969).
7. D. K. Trubey, "A Survey of Emperical Functions Used to Fit Gamma-Ray Buildup Factors," ORNL-RSIC-10 (February, 1966).
8. M. Abromowitz and I.A. Stegun, Handbook of Mathematical Functions AMS.55, U.S. Government Printing Office (1964).
9. E.A. Straker, "Time-Dependent Neutron and Secondary Gamma-Ray Transport in an Air-Over-Ground Geometry Volume II, Tabulated Data," ORNL-4289, Volume II (1968).
10. E. Storm and H.I. Israel, "Photon Cross-Sections from .001 to 100 MEV for

elements 1 thru 100," LA-3753, Los Alamos Scientific Laboratory (Nov 1967).

11. C.A. Stevens and R.R. Schaefer, "Neutron Induced Electrical Sources," AFWL-TR-69-8, Gulf General Atomic Incorporated (1968).

12. C. A. Stevens and W.H. Scott, Jr., "Neutron Induced Electrical Sources II," AFWL-TR-69-60, Gulf General Atomic Incorporated (1969).

13. C.R. Hale. To be submitted as a thesis in partial fulfillment of the requirements for the degree of Doctor of Science from the Air Force Institute of Technology.

14. W. R. Graham, Rand Corporation, private communication. This is an informal paper describing a semi-emperical formula for average forward electron ranges. It is to be published in the future as an Electromagnetic Pulse Theoretical Note.